PolyCE

Post-Consumer High-tech Recycled Polymers for a Circular Economy

Project Duration:	**01/06/2017 - 31/05/2021**
Deliverable No.:	**3.2**
Deliverable Title:	Product clustering for improved collection, sorting and reprocessing and optimized recycling economics, high purity PCR plastics streams and uptake
Version Number:	v02
Due Date for Deliverable:	**31/12/2019**
Actual Submission date:	**27/12/2019**
Lead Beneficiary:	**Katholieke Universiteit Leuven**
Lead Author:	A.T.P. Boudewijn J. R. Peeters J.R. Duflou D. Cattrysse
Deliverable Type:	R
Dissemination Level:	PU
Lead Author Contact:	A.T.P. Boudewijn KU Leuven e-mail: alexander.boudewijn@kuleuven.be

Contributing Partners
List partners and / or co-authors contributing to this Deliverable

Luca Campadello (ECODOM)

Alessia Accilli (ECODOM)

Nazarena Vincenti (ECODOM)

Arthur Schwesig (MGG Polymers)

Perrine Chancerelle (TU Berlin)

This project has received funding from the European Union's Horizon 2020 research and innovation programme under grant agreement No 730308

Summary

In this report, the work carried out to address Task 3.2 of the PolyCE project is described. The aim of the task is to improve the quality of recycled plastics through clustering strategies. Such a strategy is a policy for treating products or their components jointly or avoiding to do so in a material recovery facility. This research aim is addressed through gathering data regarding material composition of products (Task 3.1). Optimization methods are then developed for material sorting. Subsequently, feature engineering techniques are derived to quantify how efficiently distinct product components can undergo joint treatment. The methods are illustrated by means of case studies for the cooling and freezing equipment, large household appliances and small household appliances waste streams. This results in recommended clustering policies for these WEEE categories.

Contents

1 Introduction

1.1 Motivation

An estimated 4 million tonnes of waste electric and electronic equipment was collected in the European Union in 2016 [1]. WEEE comprise a broad range of products. Its material composition is complex and difficult to quantify. It is estimated that metals and plastics account respectively for roughly 60 wt% and 15 wt% [2] of WEEE. The European Commission introduced Directives 2002/96/EC and 2012/19/EC, in which targets for WEEE recycling and recovery are documented [3].

To achieve the material recovery targets of Directive 2012/19/EC, the recovery rate of the plastic fraction of WEEE should be increased. However, the complexity of this fraction imposes a challenge for Material Recovery Facilities (MRFs). Currently, metals are separated from WEEE using magnetism and eddy currents and recycled with high recovery rates, whereas most of the plastic fraction of WEEE is used for energy recovery [4, 5]. The introduction of Directive 2012/19/EU further complicated matters, as Persistent Organic Pollutants (POPs) requirements are now below measurable values for brominated flame retardants [6]. The aim of Task 3.2 of the PolyCE project is to address these challenge by incorporating *clustering strategies*. Roughly speaking, these are guidelines for the joint treatment of distinct product (or product component) categories prevalent in WEEE. Proper clustering strategies can limit the degree of contamination in output streams. Furthermore, they can limit the mixing of difficult to separate and incompatible materials. Thus, clustering strategies have the potential to significantly improve the quality and quantity of output materials of MRFs, thereby improving the WEEE plastics recycling rate.

1.2 Problem statement

This report documents a data-driven approach to tackle the problem described below. The proposed solution is illustrated in Figure 1.1. This figure also reveals the interconnectedness of the research questions.

Problem. Can the quantity, quality and financial gains of materials recovered from WEEE be improved using intelligent clustering strategies?

This problem is subdivided into Problems a, b and c as described below.

Problem a. Can a statistically sound overview of the current WEEE waste flows be obtained?

Problem b. Can the operations carried out in a recycling facility be modeled realistically and can the obtained model be used for optimizing performance indicators?

Problem c. Can product (component) clusters that, when treated jointly, improve the output of the recycling facility be identified?

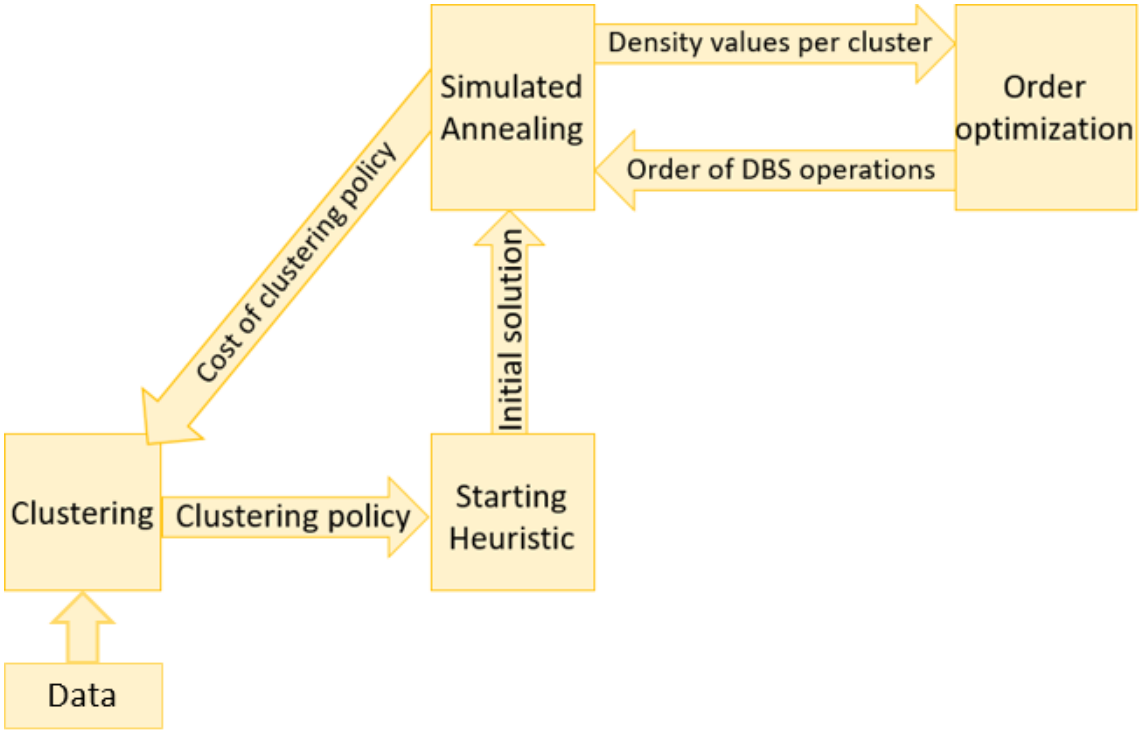

Figure 1.1. Overview of proposed solution

1.3 Placement of Task 3.2 in the PolyCE Project

The aim of Task 3.2 is to improve the quality of recycled plastics from WEEE through clustering strategies. This aim is achieved through data mining. Availability of appropriate data is therefore pivotal. The required data are the output of Task 3.1 [7], in combination with data available from prior projects carried out by KU Leuven [8]. When needed, the database is augmented by findings from literature. The results of Task 3.2 are directly applied in the demonstrators in Work Package 7. Occasionally, sophisticated insights regarding polymers (chemical properties, prices, industrial purity requirements) are required. These are estimated using results from Work Package 4.

1.4 Structure of the report

In this report, the establishment of promising clustering strategies is outlined. The main contributions presented are the methodologies for product clustering and subsequent material separation. The remainder of this report is structured as follows: In Chapter 2, an overview of material separation technologies is provided. For each technology, its target polymers are also indicated. In Chapter 3, the data available during the task is presented and the Problem is addressed. Chapter 4 is devoted to the optimization of the further separation of each cluster (Problem b). Problem c is addressed in Chapter 5. Emphasis is on the derivation of clustering strategies. In Chapter 6, the obtained methods are illustrated by means of a case study. The data is augmented by modeling assumptions for this purpose. Finally, Chapter 7 contains concluding remarks and suggestions for further research.

2 Material Separation Technologies

2.1 Introduction

Separated plastic particles have a higher resale value than a mixed plastic waste stream. Sorting is therefore an important step in plastic value recovery. A technique that can be used to isolate a plastic from a waste stream is referred to as a **sorting process**. In this section, the most important types of sorting processes are discussed. The classification is based on those presented in [9, 10]. In [11], the optimal flake size for waste in various sorting processes is determined. Table 2.1 provides an overview of the most prominent techniques in industry for plastic sorting.

Method	**Used to sort…**	**Properties**	**Instances**	**References**
Manual sorting	Components	Observable		
Density-based	Homogeneous flakes	Density; Settling velocity	Float/sink Wet/dry jig Centrifuge Hydrocyclone	[10, 12, 13] [10] [9, 10] [9]
Surface properties	ABS - remainder HIPS - remainder PP - remainder PET - PVC	Hydrophobia	Froth flotation	[13]
Optical	Identification; Contamination detection	Light emission	(DE-)XRT Polarized light UV light NIR	**[14, 15]**

Table 2.1. Overview of separation methods

Benefits of density-based sorting methods are their cost-efficiency and simplicity [9]. As a consequence, this technique is the most widely used for sorting streams of (nearly) homogeneous plastic flakes. For these reasons as well as the availability of data, the focus in this report is on density separation as the main separation technology.

2.2 Density-Based Sorting

Density-based sorting (DBS) is a set of techniques used to separate shredded flakes of materials using the difference among the materials' densities. Some ostensive material properties are directly related to the material's density. Namely, whether or not the material in question sinks in a liquid or pressured air. The velocity with which flakes of the material move or accelerate in a liquid in motion is also directly related to the density. These relations are exploited in DBS.

Unfortunately, DBS performs poorly on polyolefins. PVC and PET cannot be separated by DBS, as their densities do not differ significantly. Furthermore, the densities of plastics in WEEE and ELV are often altered due to the use of fillers or additives. This may cause DBS to perform poorly. To properly carry out density separation, the following information is required:

- A decent understanding of the waste stream's material composition;

- Knowledge of the densities of the involved materials. Particularly, whether or not the target material has a density that is either significantly lower or higher than the densities of all other involved materials. Figure 2.1 contains the typical density ranges per polymer. This figure is taken from [12].

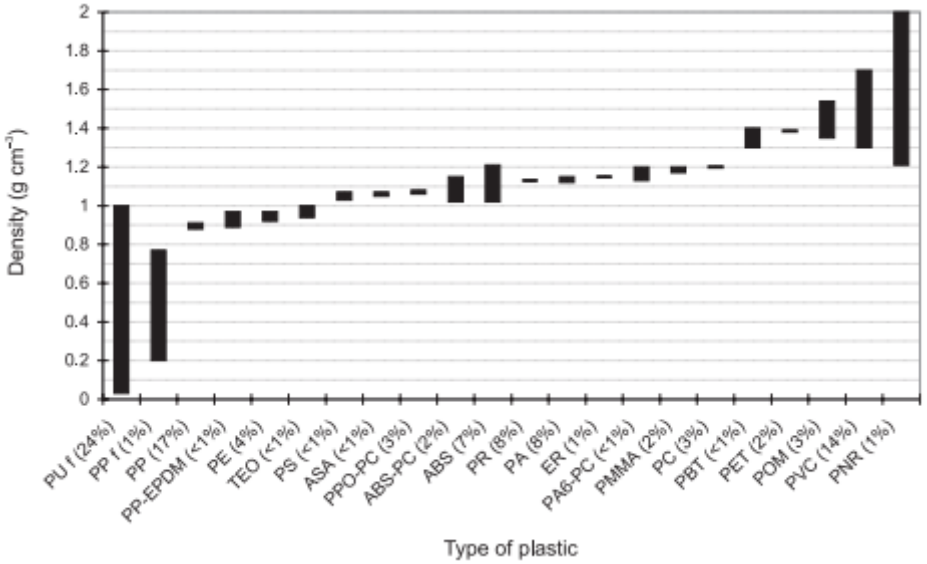

Figure 2.1: Density range per polymer [12]

In [3, 5], methods are proposed to forecast the composition of WEEE waste streams. This research focusses on long-term time horizons. In [4], a similar model is presented, with an emphasis on the continuously changing nature of ICT equipment. An overview of densities of different plastic types is provided in [11, 12]. In the remainder, it is assumed that the density of the target material exceeds that of the maximally dense non-target material. The methods have an analogous counterpart whenever the density of the target material is smaller than that of the minimally dense non-target material.

2.2.1 Float/Sink Method

Technique 2.1 *Given are flakes of a plastic mixture containing a target material and at least one other material. Suppose the density of the target material exceeds those of all other materials. Place the flakes in a liquid with a density in between that of the target material and that of the maximal density non-target material. The target material will sink, while all other materials will float.*

The float/sink method is carried out in a float bath, in which pumps direct the flow. Multiple float baths can be aligned in a sequence to separate multiple target materials or increase purity. The method requires prior wetting (e.g. friction washing) of the particles to avoid flocculation and/or the attachment of air bubbles to the flakes.

2.2.2 Hydrocyclone and Centrifugal Sorting

Technique 2.2 *Given particles containing a target material and at least one other material. Suppose that when put into motion, the target material attains a velocity sufficiently*

distinct from the other materials. Create a motion that pressures the target material to a different position than the remaining materials.

Remark 2.3 Two machines used to implement Technique 2.2 are:

- **The hydrocyclone**
  A hydrocyclone is a cylindrical body with a conic end with a tangential entrance. Water is pumped into the hydrocyclone in an accelerated spinning vortex. Particles with a higher (average) density move faster than those of lighter density. Thus, the vortex forces heavy fractions to the outside of the hydrocyclone, and light fractions to the center. The lighter fraction is then discharged through an overflow drain.
- **The centrifuge**
  A centrifuge is a double-cone in which a liquid rotates at high speed. Particles are thereby positioned in the centrifuge in clusters of similar densities.

Remark 2.4 An implementation of density-based separation using velocity is the Kinetic Gravity Separator (TU Delft, [16]). Particles are released in a rotating tank. The heavier fractions sink faster and thereby end up in different compartments of the tank.

2.2.3 Jigging

Technique 2.5 *Given are particles containing a target material and at least one other material. Also given is a (perforated) bed. Force a pulsed water stream through the bed. Feed the particles onto the bed in a water stream. The pulse will push the lighter fraction(s) upwards. The particles will thereby form (possibly more than two) layers of similar densities. Separate the layers using vibrating plates.*

Remark 2.6 An implementation of the wet jig is the Wilfley wet shaking table. Particles are released unto a diagonal table. Water is pushed upwards on the table. Heavier fractions move down the table. Lighter fractions are carried upwards by the water.

Technique 2.7 *The dry jig is analogous to wet jig, but with a gas instead of a liquid.*

3 Data Gathering and Management

3.1 Polymeric and Color Composition Product Components

3.1.1 Data Collection and Measurement Methods

ECODOM provided samples from WEEE products by cutting. Additional samples were available from previous research at KU Leuven [8]. There were two categories of samples: *disks* and *batches*. Disks of diameter roughly 55mm taken from particular product components by drill, as depicted in Figure 3.1. Detailed meta-data was gathered for each disk and each disk was analyzed individually. Batches (of roughly 5 Kg) of flakes taken from product categories after shredding were also provided. Such batches were preprocessed by manually removing contaminants (wire, aluminum, wood, other non-plastics). Subsequently, a subsample of 1Kg per batch was taken (following the protocol outlined in Section 3.1.2). This subsample was subsequently reduced in size to flakes with diameter of roughly 3mm. Measurements were carried out on these spheres. Figure 3.2 shows flakes before and after size reduction.

(a) (b)

Figure 3.1. disk sample: (a) refrigerator from which sample was taken. (b) sample.

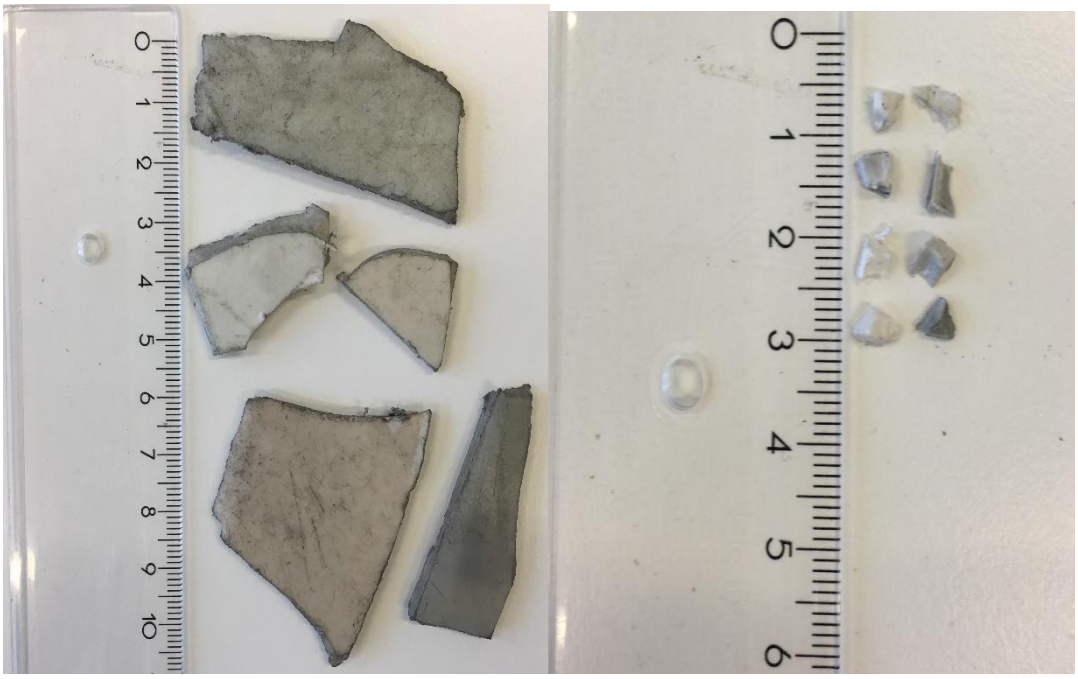

(a) (b)

Figure 3.2. Flakes (from washing machine drums) (a) before shredding (b) after shredding

All samples were analyzed by Attenuated Total Reflectance Fourier Transform Infrared Spectroscopy (ATR FTIR) using a Thermo Scientific™ Nicolet™ iS™ 5 FTIR Spectrometer. The resulting spectra were inspected and matched to reference spectra using the Thermo Scientific™ OMNIC™ 9 software package. Based on the obtained spectra, each sample was assigned a comprising material by matching it with a reference database. A database of 88 reference spectra of WEEE plastics was used that contains verified reference spectra originating from WEEE. If, for some spectrum, the closest match with any reference spectrum had a matching percentage below 80%, then the measurement was discarded. This led to reliable classifications regarding base polymers. Obtained results were occasionally verified by measuring the density of the involved sample in a float-bath. X-Ray Fluorescence (XRF) was carried out using an OXFORD™ X-MET3000 TXR+ handheld XRF analyzer to determine the presence of bromine. Colors were recorded using a computer vision system under development at KU Leuven. Colors were recorded by inspection. Material densities were measured using a lab-scale float bath, using $1{,}834$ reference samples.

3.1.2 Composition of WEEE streams

Data regarding the material flows along the EEE/WEEE value chain were documented in Task 3.1 [6]. Statistical models of future waste streams were derived and applied to case studies in [8, 19, 20, 21]. In particular, in [21], sampling and characterization protocols to assess the plastic content of small WEEE (sWEEE) in France is proposed. These forecasting methods are incorporated in an optimization framework and applied to a case study in [22]. In [23], sorting techniques are applied to identify the composition of sample WEEE streams. Finally, [24] assesses many aspects of the WEEE stream composition, namely the most prevalent products (by weight); their ease of disassembly and their material composition. In this report, the quantification of WEEE streams is mainly based on [6, 22]. Future research into the

composition of WEEE streams could incorporate the protocols from [20] with the modeling methodology from [8, 17, 20, 22, 23] to quantify future WEEE compositions.

In [7], (W)EEE is subdivided into four categories, namely: Cooling and Freezing equipment (C&F); Large Household Appliances (LHA); Televisions and Screens (TV&S) and Small Household Appliances (SHA). The tonnage and proportion (rounded to the nearest decimal) of each of these categories in the WEEE stream in Europe in 2016 is given in Table 3.1. Table 3.2 contains data regarding the mass proportions of product types in collected WEEE streams.

	WEEE collected tons	WEEE collected Proportion (%)
C&F	662,485	19.5
LHA	1,158,890	34.0
TV&screens	539,735	15.8
SHA	1,044,472	30.7
TOT	**3,405,582**	

Table 3.1. WEEE collected in Europe in 2016 [7].

C&F		LHA		TV&S	
Fridges	93%	Dishwasher	12%	CRT	90%
		Kitchens	9%		
Freezers	6%	Washing Machines	72%		
		Dryers	1%	FPD	10%
Air Conditioner	1%	Heating, Ventilation	4%		
		Microwaves	1%		

Table 3.2. Mass proportions of key product categories per category in WEEE collected in Europe in 2016 [7].

In [22], a study of a local MRF in Spain in 2016 revealed that the most prevalent (in terms of mass) product categories in the SHA stream include vacuum cleaners, coffee makers, printers, irons and radio cassettes. Furthermore, the article states that, in terms of mass, vacuum cleaners are roughly half comprised of plastics. For coffee machines, the proportion of plastic mass is roughly70%. For irons, this percentage is below40%. This makes vacuum cleaners coffee makers and printers key sources of plastic in the SHA stream. These findings were corroborated by measurements performed by ECODOM within the scope of PolyCE Task 3.1 in the Milan metropolitan area in January 2019: at end of December 2018/ begin of January 2019, ECODOM performed three sampling campaigns in two different WEEE pre-treatment plants in Italy to understand the camposition of the current SHA waste stream. The results of the sampling campaigns (Table 3.3) show that printers, coffe machines and vacuum cleaners are the most revelant products (by weight) in the current SHA flow.

SHA products	Sampling n.1	Sampling n.2	Sampling n.3
	Presence in current SHA flow (% by weight)		
Printers - multifunction	12,1%	9,2%	5,2%
Printers - only	1,6%	15,5%	3,0%
CD/DVD/VHS readers	3,7%	1,3%	4,9%
Vacuum cleaners – with wheels	3,5%	3,7%	3,2%
Coffee machines	3,6%	4,4%	3,1%
Vacuum cleaners – electric brum	0,8%	3,2%	3%

Table 3.3. Results of ECODOM's sampling campaign for SHA

The overall polymeric composition of WEEE was documented by MBA Polymers (currently MGG Polymers; see [24]) and is depicted in Figure 3.3.

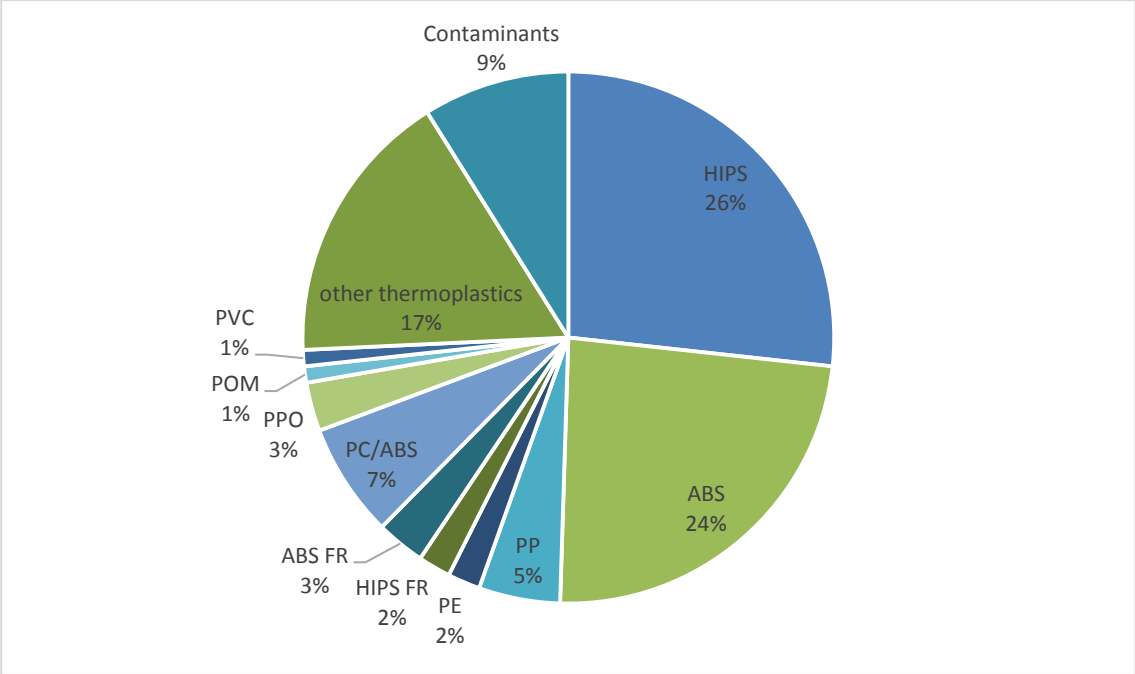

Figure 3.3. Composition of WEEE plastic stream [24]

3.1.3 Data storage and structure

3.1.3.1 Disks

Information regarding the origins of each disk was stratified by EU directive 2012/19/EU [6], UNU-key [25], HS-code [26], brand, product, component and material (the measurement result). The obtained classification is depicted in Figure 3.4. Further meta-data gathered was the collection location and date and if available, the country and year of production. Each disk was labeled with a unique identification number. Hence, data regarding each individual disk is recorded and the disk corresponding to a data point is readily available for reference.

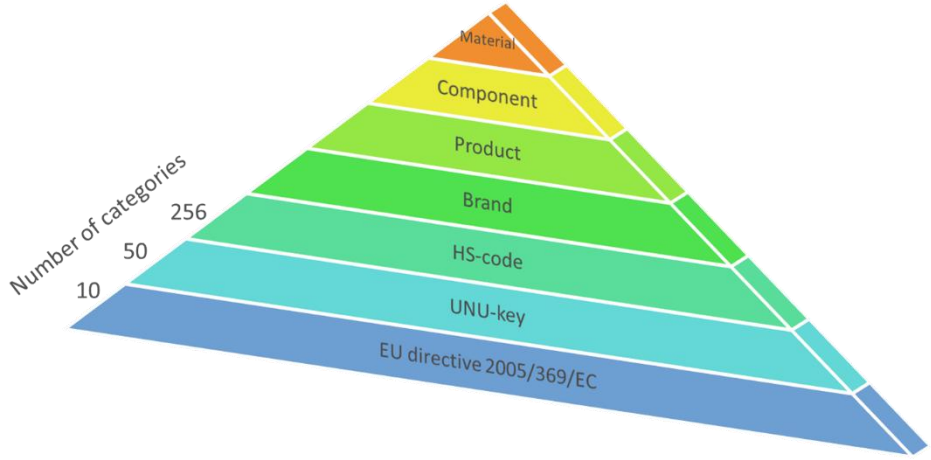

Figure 3.4. Classification of disks by meta-data

3.1.3.2 Batches

For batches, metadata was gathered to capture how the sample was comprised and processed before collection. This includes the product categories treated and the separation and size reduction technologies applied to them. A template of a meta-data sheet containing the data requested with each batch sample is provided in Appendix A.

3.1.2. Subsampling Method for Batches

A subsampling method was developed to take a representative subsample of roughly 1Kg for FTIR analysis from a larger 5Kg batch of flakes. The method is based on [27, 28, 29]. Subsampling was applied because a sufficient amount of flakes were still required for testing a computer vision set-up (part of PolyCE Task 4) and for archiving. Batches were stored in plastic bags, hence, larger pieces tended to be more densely concentrated in the upper-half of the bags. To still obtain a representative sample of the entire batch, the following protocol was developed:

1. Spread out all the flakes on a flat surface;
2. Stir the flakes by hand for two minutes;
3. Spread out all the flakes in a square (as flat as possible); Typically, such a square had edges of length $50mm$;
4. Draw a regular grid in the square directly, or using rope;
5. Start at grid $(0,0)$; take one sample from this grid, then move on to grid $(0,1)$ etc. until the selected sample has reached 1Kg.

This procedure was applied to take a subsample that is as representative of the sample as possible. The procedure is illustrated in Figure 3.5. The selection of the grid sizes is left to the researcher, as it depends on the size of the square. The optimal grid size satisfies the condition that each grid is sampled exactly the same number of times exactly when the mass of the subsample reaches 1Kg. While this is hard to anticipate fully, it provides a heuristic for grid size selection.

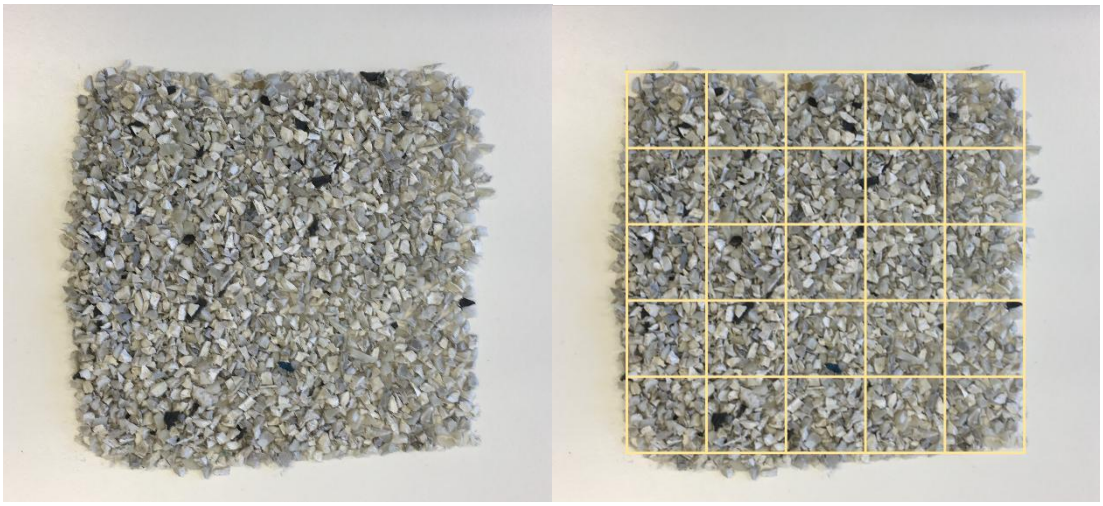

(a) (b)

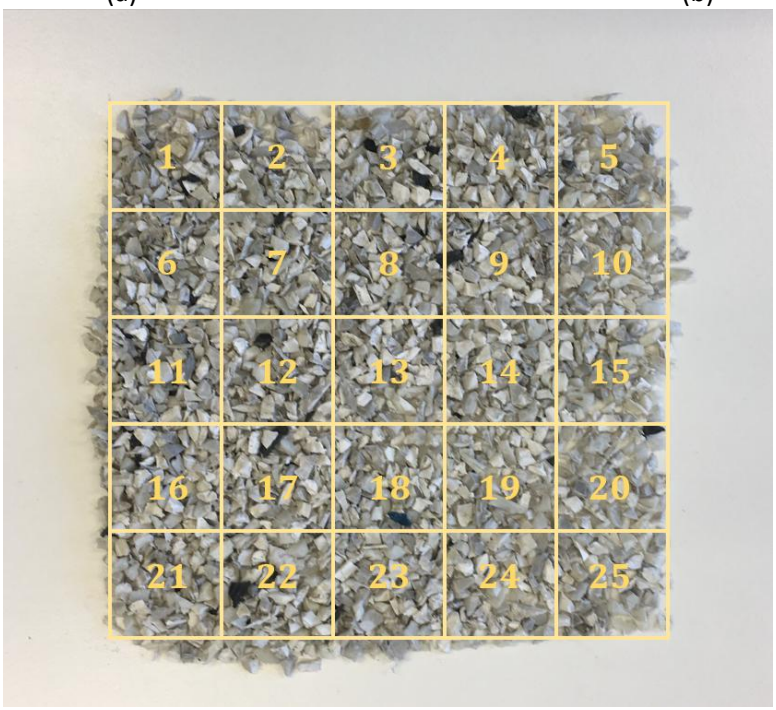

(c)

Figure 3.5. Subsampling procedure (a). Arrange sample into a flat square. (b). Draw a regular grid on the square (for instance, using rope and duct tape). (c). Label the grids. Select one sample at random from grid 1. Subsequently, select one from grid 2 and so on. Once a sample has been taken from grid 25 and the capacity of the subsample is not reached, restart at grid 1.

3.1.4 Sampling Theory

3.1.4.1 Material composition hypothesis testing

For each stratum i of disks or for i some batch, a number n_i of samples are analyzed. The results fall into a collection of k distinct materials. Thus, each stratum i or batch i corresponds to a vector of observations X_i of the form in equation (3.1).

$$X_i = (x_{i,1}, \dots, x_{i,k}) \tag{3.1}$$

Suppose the population distribution is P_i. For a given null-hypothesis $H_0: P_i = a_i$, the Pierson statistic is now defined as in equation (3.2).

$$C_{n_i}^2 := \sum_{j=1}^{k} \frac{\left(x_{i,j} - n_i a_{i,j}\right)^2}{n_i a_{i,j}} \tag{3.2}$$

The following result is proven as Theorem 2.9 in [30].

Theorem 3.1. If the vectors X_i are multinomially distributed with parameters n_i and $a = (a_1, \dots, a_k) \geq 0$, then the sequence $C_{n_i}^2$ converges (*in distribution*) to the χ_{k-1}^2-distribution.

Theorem 3.1 is commonly referred to as the "Chi-Squared test" and provides a method to assess the reliability of the sampling results. The shortcoming is that a null-hypothesis is required. However, reliable estimations by experts can function as null-hypothesis. Given a null-hypothesis $H_0: P_i = a_i$, the observed data X_i serves as the alternative hypothesis $H_1: P_i = X_i$. Note that Theorem 3.1 involves asymptotic behavior of the test statistic. As a consequence, the method becomes more reliable as more data becomes available. To adequately compute a minimal sample size for the chi-squared test, three additional parameters have to be available: the effect size, the (threshold on the) significance level and the power. These are discussed below. These definitions are considered common knowledge, and an explicit reference is omitted. The reader is referred to any textbook on basic statistics for more background information (for instance, [31]).

Definition 3.2. Given a null hypothesis $H_0: P_i = a_i$ and an alternative hypothesis $H_1: P_i = X_i$, the **effect size**, denoted by w, is given by equation (3.3).

$$w = \sqrt{\sum_{j=1}^{k} \frac{\left(X_{i,j} - a_{i,j}\right)^2}{a_{i,j}}} \tag{3.3}$$

The effect size is a measure of discrepancy between the postulated and measured results. In [32], effect sizes of 0.1, 0.3 and 0.5 are considered small, medium and large, respectively.

Definition 3.3. A **type-I error** is the error made when a true null-hypothesis is rejected. A **type-II error** is the error made when a false null-hypothesis is accepted.

Definition 3.4. Given a null-hypothesis $H_0: P_i = a_i$, and an observation b_i, the **significance level** or ***p*-value** is defined through equation (3.3).

$$p := 2 \min_{\mathrm{j}} \{P\left(a_{i,j} \leq b_{i,j}\right), \quad P\left(a_{i,j} \geq b_{i,j}\right)\} \tag{3.4}$$

If the p-value is small, then the probability that the observations stem from the distribution in the null-hypothesis is large. Thus, a small p-value means that the observation very likely comes from this distribution, and the null hypothesis is most likely true. In practice, a threshold level α is usually fixed for the p-values to be encountered. The threshold α is a threshold on the probability of making a type-I error. A common threshold is $\alpha = 0.01$ (so that the null-hypothesis is rejected if $p > 0.01$).

Definition 3.5. Given a null-hypothesis $H_0: P_i = a_i$, and an alternative hypothesis $H_1: P_i = b_i$, the **power** of the test, denoted by $1 - \beta$, is the probability that H_0 is accepted, given that H_1 is true.

A commonly used threshold on the power is 0.9. For $\alpha = 0.01$. A table that can be used to determine an optimal sample size is included in Appendix A.2. This table is taken from [32]. The degrees of freedom and significance level are fixed in the table. The columns contain sample sizes and the rows contain effect sizes. The values in the table correspond to powers. Thus, the user can look at the row of the desired effect size, look for the desired power in that row and read off the required sample size from the corresponding column. Obviously, the underlying function is a built-in routine in many software packages as well. In [32], several such tables are provided for different combinations of α and the degrees of freedom.

Example 3.6. Suppose FTIR measurements of LCD monitor back covers can fall into one of the categories {ABS, ABS/PMMA, HIPS, HIPS/PPE, PA, PC/ABS, PP, unknown}. The aim is to test the null hypothesis

$$H_0: X_{LCD\ M} = (0.5 \quad 0 \quad 0.3 \quad 0 \quad 0.2 \quad 0 \quad 0 \quad 0)$$

With a significance level of 0.01, a medium effect size of 0.3 and a power of 0.9. The smallest sample size needed to test the hypothesis given the parameters can now be determined as follows. Since we have a vector in $\mathbb{R}^8$, we have seven degrees of freedom. Table A.2 contains values for α fixed at 0.01 and the degrees of freedom fixed at 7. Hence, take the column of 0.3 (the desired effect size). In this column, look for the value 90 (the desired power). The smallest value in the column that is larger than 90 is 94. Now take the sample size on the row containing this value of 94. The conclusion is that a sample size of 300 LCD monitors is required to test the null hypothesis.

In practice, the effect size is computed once the measurements are carried out. A good approach is then to estimate the effect size beforehand (based on confidence in the null hypothesis); choose a slightly larger power than needed; take the sample size corresponding to the estimate and update the parameters if necessary when reporting the results.

An advantage of the outlined method to determine the minimal sample size is that it does not rely on the population size, since data regarding the population size is not directly available and would have to be estimated from other research findings. Furthermore, the resulting sample sizes tend to be manageable. A disadvantage is that it requires a specific null-hypothesis. In the current study, due to a lack of data as well as previous findings, measurements will be treated as distribution functions. Once more data becomes available, the presented findings can be used as a null hypothesis along with the outlined method to determine the required sample size. Methods to incorporate results from prior studies in a newly established data set are detailed in [33].

3.1.4.2 Compliance testing

A more trivial method exists to determine an appropriate sample size for binary random variables (for instance, when testing whether or not a stream complies with given legislation). This is outlined here. It is based on [34] in which methods are also described to generalize the reasoning in the prevalence of stratified populations. Suppose that P ist he population proportion of compliant instances. Denote by p the sample proportion, thus

$$p \coloneqq \frac{1}{n}\sum_{k=1}^{n} y_k$$

where n ist he sample size and

$$y_i = \begin{cases} 0, & if\ sample\ i\ is\ compliant \\ 1, & otherwise \end{cases}$$

Now, p is an unbiased estimator for P. Likewise,

$$s^2 \coloneqq (1-f)\left(\frac{1}{n-1}\right)p(1-p)$$

Where $f = n/N$ with N the population size is an unbiased estimator for the population variation. The sample coefficient of variation therefore becomes

$$cv_y \coloneqq \frac{s_y}{p} = \sqrt{(1-f)\left(\frac{1}{n-1}\right)\left(\frac{1-p}{p}\right)}$$

A $\alpha\%$ confidence interval (C.I.) for the population mean P can now be computed using these estimators through equation (3.5).

$$I_{95}(P) = p \pm z_{\alpha/2} \cdot cv_y \tag{3.5}$$

with $z_{\alpha/2}$ the z-score corresponding to a confidence interval of $\alpha\%$ (for instance, for $\alpha = 95\%$, $z_{\alpha/2} \approx 1.96$. Suppose a margin of error of r is required the C.I. should then satisfy

$$z_{\alpha/2} \cdot cv_y < r$$

Or, equivalently,

$$z_{\alpha/2} \cdot \sqrt{\left(\frac{N-n}{N}\right)\left(\frac{1}{n-1}\right)\left(\frac{1-p}{p}\right)} < r$$

From this inequality, n can be computed for given N, p and r. Again, in practice, an assumed value p^* may be chosen for p. The sample statistic p can then be computed after samle taking. If p is significantly different from p^* (so that the derived value of n is no longer valid), the process is iterated with the sample statistic p. This process may be repeated until a valid sample has been taken.

3.1.5 Results

3.1.5.1 Flakes

Based on the results from Section 3.1.2, the data collected in the form of disks was as visualized in the dendrograms in Figures 3.6 through 3.8. Numbers in the leaves of these dendrograms represent the number of samples taken for the corresponding class. An additional sampling campaign for SHA was carried out in the fall of 2017, but the results were inconclusive as the stream was too diverse (the comprising products were too diverse for statistically sound samples of product classes).

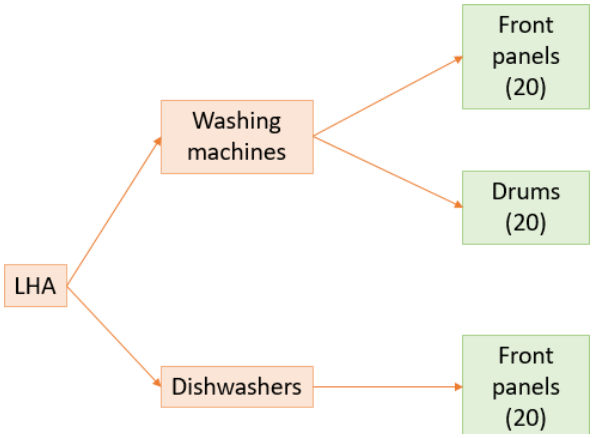

Figure 3.6. LHA sampling campaign

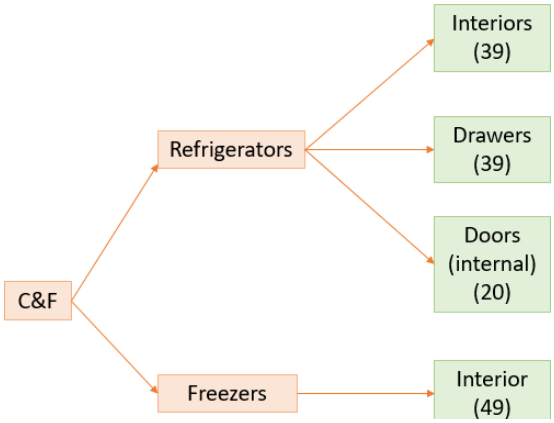

Figure 3.7. C&F Sampling campaign

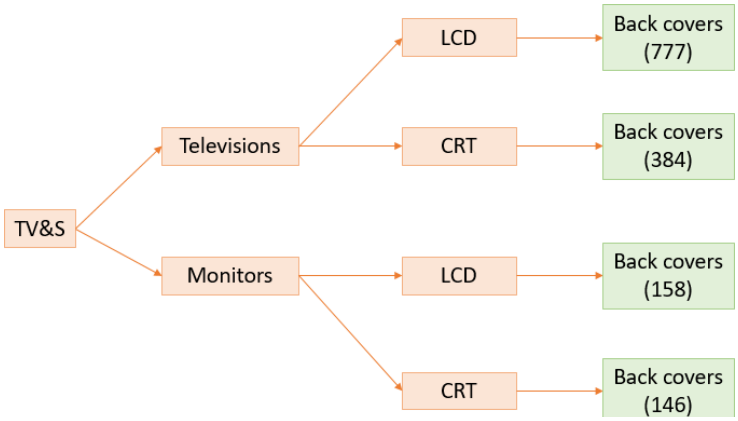

Figure 3.8. TV&S sampling campaign

Results concerning polymeric and color composition are provided in the *heatmap* in Figure 3.9. In this figure, dark shades correspond to high concentrations of the polymer or color in the row that are present in the product component on the corresponding column.

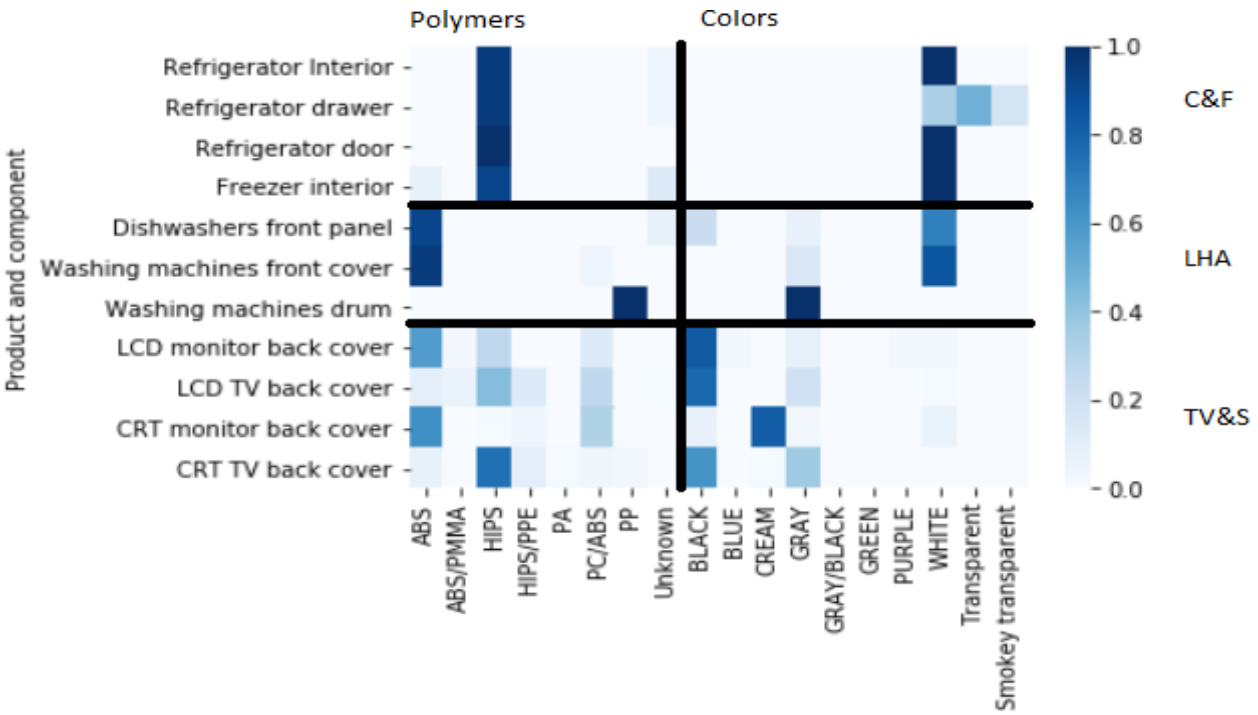

Figure 3.9. Heatmap of main polymers and colors per product component

3.1.5.2 Batches

Experiments were carried out with batches as documented in Table 3.4. Results are depicted in Figure 3.10.

Category	Product	Component	No. of trials	No. valid spectra
LHA	Washing machine	Entirely	1	48
	Washing machine	Drum	1	47
C&F	Refrigerator	Entirely	2	55; 68
	Refrigerator	Transparent drawers	1	42
	Refrigerator	White drawers	1	35
SHA	Printers	Entirely	1	69
	Coffee machines	Entirely	1	63

Table 3.4. Sampling campaign for batches

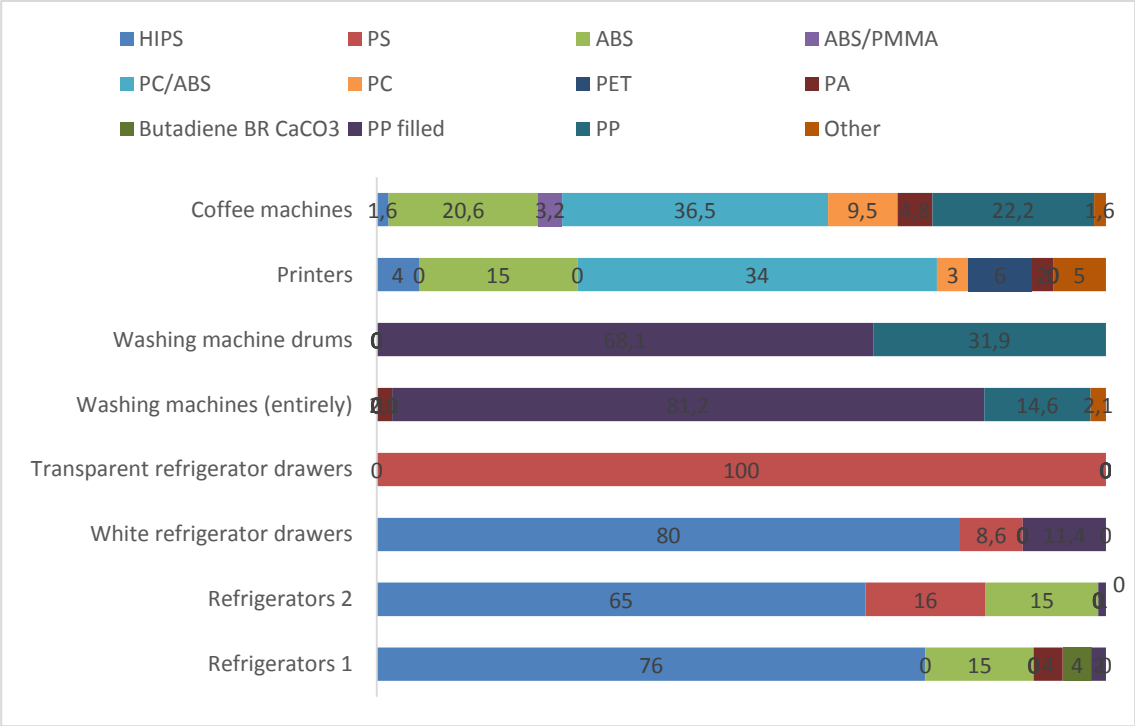

Figure 3.10. Results of batch analyses

3.1.6 Conclusion and Discussion

In this chapter, methods were outlined for collection, subsampling and analyzing of data regarding WEEE. Furthermore, guidelines were provided for deriving an appropriate sample size and a proper hierarchical data structure for storage and aggregation. All these tasks were centered around samples in either the form of disks or the form of batches flakes after size reduction. Analysis results were documented for disks and batches, showcasing the polymeric (and in the case of disks, also color) composition of involved product components.

Regarding the results, a few initial observations are easily made. First of all, Figure k+8 indicates that washing machine drums contain significantly more unfilled PP when compared to shredded flakes of entire washing machines. Unlike fillers in the washing machine stream, which were typically talc or $CaCO_3$, fillers in washing machine drums were hard to detect using FTIR. However, filled PP was easily removed from unfilled PP using density separation. Thus, washing machine drums form a reliable source of unfilled PP.

Furthermore, it is evident that washing machine drawers consist mainly of (HI)PS. Flakes from entire shredded refrigerators, on the other hand, often contain ABS and PA and can be polluted by rubbers. As ABS and HIPS share a density range, pollution by ABS is also undesirable. Again, this makes refrigerator drawers a particularly interesting source of recycled (HI)PS. These findings are further corroborated by the findings regarding disks. These show that most of the main plastic components of cooling and freezing equipment consist of (HI)PS. However, as drawers are easily removed, doing so can significantly reduce the risk of contamination.

3.2 Material Recovery Facilities

The techniques outlined in Chapter 2 can theoretically all be of use when separating polymers. However, discussion with PolyCE partners (Ughent) indicated that the most commonly adopted separation methods by MRFs in practice are density-based sorting, near-infrared spectroscopy (hereafter: NIR) and colour identification. Material miscibility (when compounding) is sometimes taken into consideration. Throughout this document, it is assumed that the MRF in question has sufficient equipment for the various separation operations. That is: no investment has to be made in new equipment for e.g. NIR sorting.

It is important to note that automated systems for NIR and colour identification are most effective on a different scale than density-based sorting. For NIR and colour identification to be effective, a spectrum or image of each individual material flake has to be taken. An appropriate action must then be taken. For density separation, on the other hand, the flakes have to be sufficiently small. This is because surface area and interconnection of components may affect floating and sinking behavior of particles. A thorough review of optimal flake sizes for distinct separation technologies is available in [11, 35]. The outlined considerations regarding MRFs result in the representation of an MRF depicted in Figure 3.11.

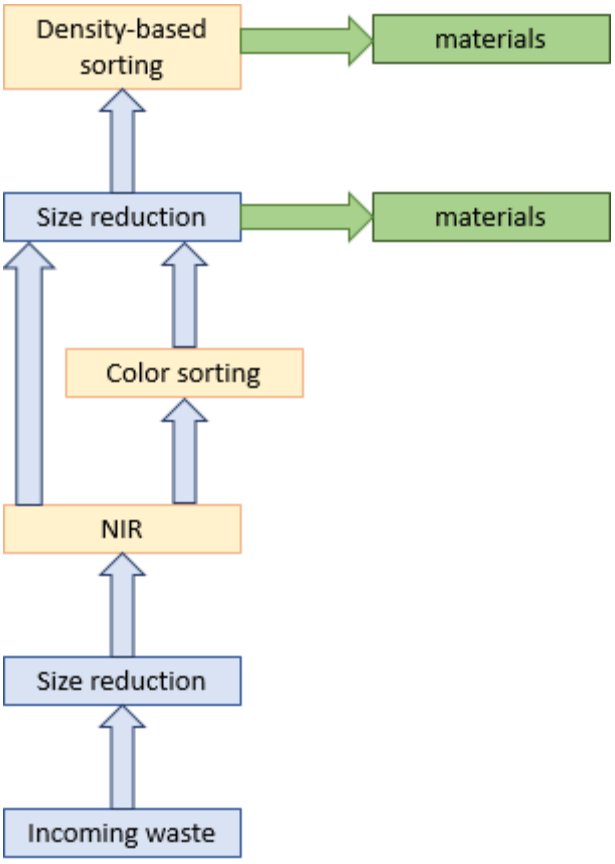

Figure 3.11. Representation of an MRF

3.2.1 Density-based sorting

3.2.1.1 Density spectra

Plastics exhibit small differences in molecular weight, chemical composition and may contain additives in different concentrations. Hence, plastics lack a fixed density value. Rather, the density a material can take on is within a range of values. To model the ranges and the likelihood that each material takes on a density within a given interval, the densities of the $1{,}834$ reference samples were measured. The results were categorized into 44 density values from $1.03\ g/cm^3$ to $1.25 g/cm^3$, in increments of $0.005 g/cm^3$, and an additional 3 density classes of $1.35 g/cm^3, 1.45 g/cm^3, 1.55 g/cm^3$. The results were then normalized, giving the proportion of samples with each density value for each material as illustrated in Figure 3.12.

In Figure 5, material density is on the x-axis. On the y-axis, there is the proportion of samples of hypothetical material, say material M (a value between 0 and 1). The curve represents the proportion of samples of material M with each given density value. Thus, the shaded area is the proportion of samples of material M with a material density between $1.225 g/cm^3$ and $1.240 g/cm^3$. The obtained density spectra for base polymers are depicted in Figure 3.13.

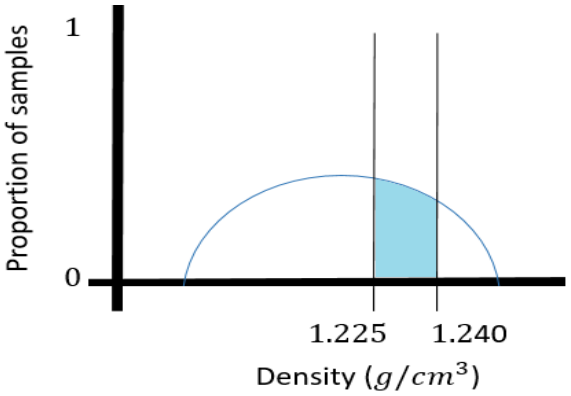

Figure 3.12. Density spectrum for a hypothetical material

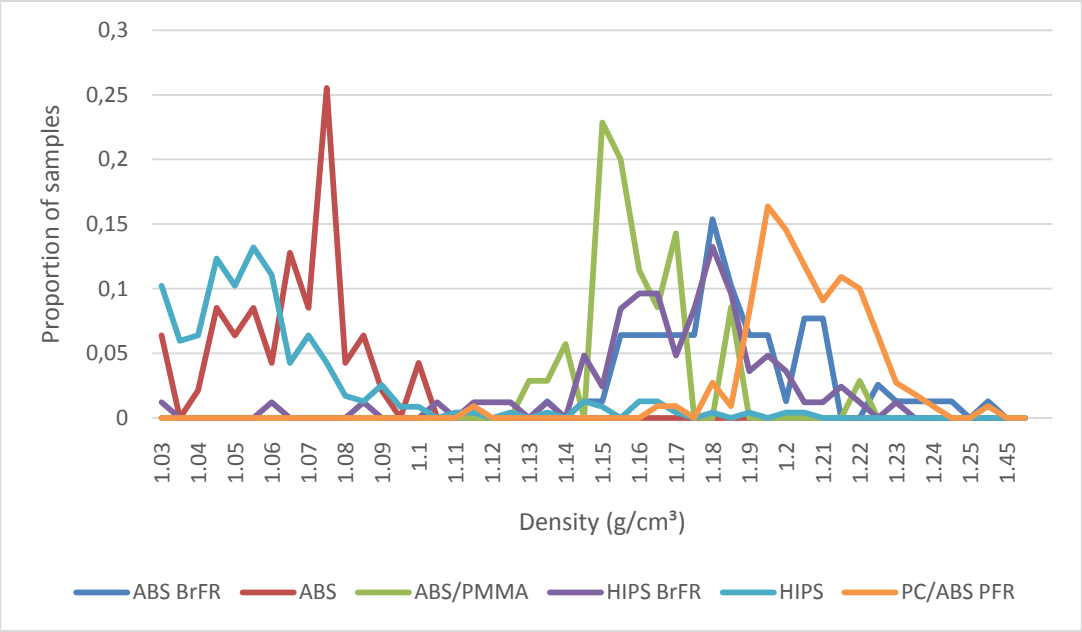

Figure 3.13. Density spectra of base polymers

3.2.1.2 Representing density-based sorting in tabular form

The first step in designing features for DBS is to derive the efficiency table (as introduced in Section 3.6.4) of this process. Consider Figure 6. Observe that two distinct materials may have overlapping density spectra. Whenever such an overlap is significant, a trade-off (Pareto front) between purity and yield is made if DBS is applied. This is illustrated in Figure 3.14.

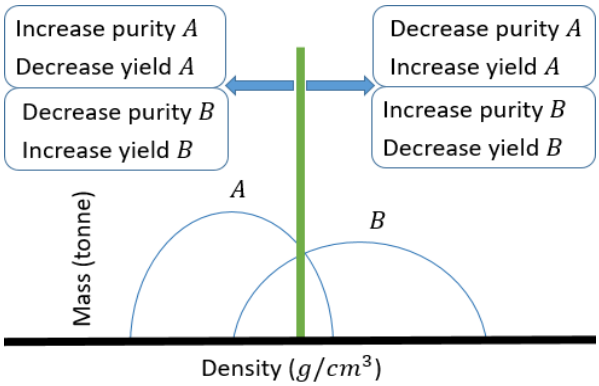

Figure 3.14. Purity/yield trade-off for density separation for hypothetical materials A, B.

The smaller the area of overlap, the less constraining the trade-off becomes. The Proportional Area of Overlap (with respect to the total area) in normalized spectra (PAO) is therefore a good metric for the effectiveness of DBS for the materials of interest. The reader is spared the somewhat meticulous formal definition of this metric. Instead, the metric is illustrated in Figure 3.15.

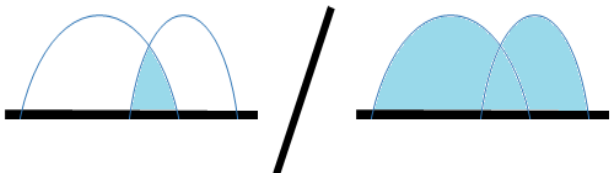

Figure 3.15. Metric for assessing the applicability of DBS.

Table 3.5 contains the PAO for all combinations of two materials for which density data was available. In the remainder, we will treat this table as an efficiency table. Note that the table is symmetric and that only the off-diagonal entries are meaningful. We will use the notation $PAO(i,j)$ to denote the PAO of materials i and j. A more complete table, where data is augmented by assumptions based on [12] is included in Appendix C.

Density overlap	ABS BrFR	ABS	ABS/PMMA	HIPS BrFR	HIPS	PC/ABS PFR
ABS BrFR	1,00					
ABS	0,00	1,00				
ABS/PMMA	0,23	0,00	1,00			
HIPS BrFR	0,54	0,02	0,29	1,00		
HIPS	0,04	0,40	0,02	0,06	1,00	
PC/ABS PFR	0,27	0,00	0,03	0,15	0,02	1,00

Table 3.5. Efficiency table for density separation (rounded to three significant figures)

The PAO is a symmetric measure for any two given materials. As outlined, it is computed for normalized spectra. In practice, density spectra are weighted by their masses in a WEEE stream. A measure can then be used to quantify the degree to which one of the materials, say m, in the input stream, say S, is polluted by another material, say m'. This quantity will be referred to as $PAO'(S,m,m')$. Its computation is similar to that of the standard PAO. However, instead of dividing the overlapping area by the union of the spectra of m and m', one should divide only by the total area of m. This is illustrated in Figure 3.6.

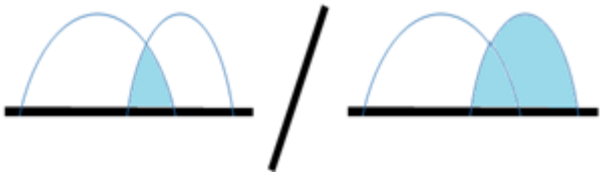

Figure 3.16. Illustration of PAO' computation

3.2.2 Near-Infrared Spectroscopy (NIR)

The discussion outlined in this session is based on internal discussion with UGhent as well as [14, 15]. NIR is a technique to separate target materials from a complex material stream based on spectral information. Typically, each NIR process targets one particular polymer. When carrying out NIR sorting, plastic flakes are placed on a conveyor belt. The flakes are then analyzed one-by-one. Depending on the analysis result, the flake is either placed in the target fraction or the non-target fraction at the end of the conveyor belt.

To separate k polymers using NIR as a sole separation technology, one would therefore require k NIR processes in series. The effectiveness of NIR in identifying particular products is hard to estimate. In [14], the efficiency of NIR is considered to be between 80 and 95%, depending on throughput. In [15] it is stated that NIR is used with the following polymers as targets, with an accuracy of 90 to 99.9%.

- PET;

- HDPE;
- LDPE;
- PP;
- PVC;
- PS;
- HIPS;
- ABS;
- PC;
- PC/ABS;
- POM;
- PA;
- PPO;
- PMMA.

However, the accuracies are highest for the separation of PET from specific other polymers (such as PVC), as these are common in the sorting of plastic bottles.

3.2.3 Colour identification

In this document, colour is taken into consideration through a distinction in recyclate prices for white and non-white plastics; see Section 3.3.6.

3.2.4 Material miscibility

Instead of separating materials, one may also aim to blend them to optimize the value of the output stream. Metrics are derived to assess the degree to which distinct polymers are miscible in [23]. The results are depicted in Figure 3.17. Here, a 'G' ("green") indicates a high degree of miscibility (maintaining physical properties). For values 'Y' and 'O', in that order, miscibility becomes reduced. The value 'R' indicates deterioration of physical properties after blending.

	ABS	HIPS	PET	PC	PMMA	PC ABS	POM	PE	PP	PA	PPE	SAN	PVC	HIPS PPE	PBT
ABS	G														
HIPS	Y	G													
PET	O	O	G												
PC	G	O	G	G											
PMMA	O	O	Y	O	G										
PC ABS	G	Y	O		O	G									
POM	O	O	R	R	R	R	G								
PE	O	O	R	R	R	R	R	G							
PP	R	R	R	R	R	R	R	Y	G						
PA	O	O	O	O	R	O	R	Y	O	G					
PPE	O	G	R	R	R	R	R	O	O	Y	G				
SAN	G	O	R	G	G	G	R	R	R	O	R	G			
PVC	G	O	R	Y	G	O	R	O	O	R	R	G	G		
HIPS PPE	O	G	R	O	O	upto 15%	R	O	O	R	G	O	R	G	
PBT	G	R	Y	Y	R	R	Y	O	O	O	R	R	R	R	G

Figure 3.17. Miscibility of different polymers [23]

3.3 Additional required data

3.3.1 Density spectra

Density spectra for some common polymers (coPP, homo PP, PS, …) are currently missing. The addition of such data could significantly improve the results of the implemented methods. Such spectra may be inferred from the literature (see, e.g. [12]).

3.3.2 Presence of contaminants

The types of contaminants that can be expected in product categories and their impact can be essential information for clustering. Examples of types of contaminants are fillers, (brominated) flame retardants, glass fibers, rubbers, etcetera. The degree of contamination can be represented as a mass percentage or pass/fail criterion. These data can be obtained through surveying WEEE preprocessors and MRFs. Obtaining insightful data regarding contaminants is a crucial part of PolyCE work package 4.

3.3.3 Industrial technologies, costs and throughput

To improve the clustering and optimization methods, knowledge regarding the technologies (sorting processes) applied and their efficiencies is required. Mainly of interest are the purity and yield of output streams for each combination of two input materials. For some process x, such data can be stored in a table with materials on both axes. Entry (i, j) in such a table contains a parameter representing the effectiveness (purity and yield of resulting fractions) with which materials i and j can be separated by process x. The parameter can be chosen based on the trade-off between purity and yield. Such a data structure is referred to as the *efficiency table of operation* x in the remainder of this report. This is illustrated in Table 3.6. An efficiency table for density separation is explicitly derived in Chapter 5.

Process x	PA	PP	PS
PA	-	-	-
PP	*Ease with which process x separates PP from PA*	-	-
PS	*Ease with which process x separates PS from PA*	*Ease with which process x separates PS from PP*	-

Table 3.6. Example of an efficiency table for a hypothetical separation process x

The sensitivity of these metrics in the presence of common contaminants is also of interest. These data can be obtained by sampling the output streams of each sorting process after providing it with an input stream consisting of just two materials. Such experiments will be performed in PolyCE work package 4. Fortunately, the clustering methodology is rather modular, such that these data can easily be incorporated when available. It can also be implemented so as to resemble the settings of a specific MRF given the appropriate information.

3.3.4 Operation costs, incineration costs, throughput MRFs

Operation costs for MRF processes could not be disclosed by partners. Estimates are included in Table 3.7. These parameters are easily altered in case more accurate data becomes available.

Operation	Unit cost $[€/tonne]$
Density-based sorting	150
NIR	200
Size reduction	150
Incineration	150

Table 3.7. Operation costs

Discussion with PolyCE partners indicated that the annual throughput of an MRF is roughly $25 \cdot 10^3$ tonnes. Data regarding the unit costs (in terms of man-power, space, energy, time) associated with each separation process are required. In the case study in Chapter 6, these costs are estimated. The same goes for incineration costs. Costs of sorting and dismantling poducts are estimated based on discussions with PolyCE partners. These costs can be broken down into several components. Each cluster requires a dedicated production line to avoid contamination. WEEE pre-processors consultation results, the main costs related to clusters implementation are due to:

- **sorting phase:** at this stage, additional costs occur to cover additional labour required (additional operators need to be employed to manually remove specific products from the traditional waste flow an to charge then the treatment line, putting for example the sorte products in the shredder);
- **storage phase**: additional storage space is required before and after the treatment activities. Before the treatment, product needs to be stocked until reaching the appropriated amount of material to be treated in batch; after the treatment, the different plastic types obtained need to be kept separately and dedicated space needs to be devoted for this in the treatement plant. Moreover, it should be taken into account that for specific cluster, as plastic drawers of fridge, the stored products occupy a considerable volume while the material is considerable low in term of plastic weight. This aspect has a considerable impact also in terms of manual work required to handle the material;
- **treatment phase:** at this stage**,** additional time is required. In fact, treatment activities in clusters are very slow compared to normal operation (considering that it is necessary to store the products, stop/clean the treatment line, reactivate the treatment line); moreover, it should be taken into account that the treatment of the products excluded from the cluster, for example dishwasher alone, can result more difficult than the one of the traditional mix (for example, buoyancy phenomenon can occur in the shredder treating plastic alone, rather than a plastic-metals mix).

Costs differ depending on the category of the product. Below, estimates are provided four three demonstrator cases (hereafter: the demonstrators): the removal of refrigerator drawers from refrigerators; the removal of drums from washing machnes; the separation of three products (coffee machines, printers and vacuum cleaners) from the laerger SHA stream. The data reported have been elebaorated also considering the feedback received from WEEE pre-processors involved in the clustering demonstrators activities (WP7).

3.3.4.1 Refrigerator drawers

The implementation of a dedicated line incurs an estimated one-time cost of €30.000 and an annual set-up cost of €500. Other costs estimates depend on throughput of the MRF and are provided in Table 3.8.

Cost factor	Unit cost (€/tonne)
Additional labour (sorting/dismantling)	100
Material handling	70
Stock management (storing costs)	100
Size-reduction	150
Total	420

Table 3.8. Costs involved in sorting

3.3.4.2 Washing machine drums

A dedicated line for washing machines requires twice the amount of space of an MRF under normal circumstances. Dismantling the washing machines requires a significant amount of time with additional labour costs of €60 to €70 per hour.

3.3.4.3 Small household appliances

The implementation of a dedicated line incurs an estimated one-time cost of €30,000 and an annual set-up cost of €500. An additional $130m^2$ to $180m^2$ of industrial space is required ($100m^2$ to $150m^2$ for storage of input SHA until a batch size is obtained; $30m^2$ for storage of output materials). At $€125/m^2$, this incurs an additional initial investment between €18,750 and €22,500. Additional labour costs are estimated at €10 to €15 per tonne.

3.3.5 Recyclate polymer values

Recyclate polymer values are currently estimated based on [36, 37]. The estimates are shown in Table 3.9. Note that transparent plastics materials are suitable for the creation of white recyclates in a masterbatch. Polymers with value 0 cannot be sold and have to be incinerated for energy recovery. Incineration costs are estimated to be €150 per tonne (regardless of the material involved).

Material	white	Coloured
ABS BrFR	0	0
ABS	1670	1670
ABS/PMMA	0	0
HIPS BrFR	0	0
HIPS	980	930
HIPS/PPE PFR	0	0
PC/ABS	2335	2000
PC/ABS PFR	0	0
PP	1000	900
CPP	1285	950

hPP	1000	900
PA	2415	2085
PC	2580	2145
PS	500	400
PET	750	625
PUR	0	0
PE	710	710
PVC	0	0

Table 3.9. Unit prices $[€/tonne]$ of polymer recyclates per color

3.3.6 Colors of plastics

Data regarding the distribution of colors in waste streams should be included in order to efficiently sort out lighter fractions. Experiments for obtaining these data are currently executed in PolyCE work package 4.

4 Optimizing Material Recycling Facilities for Given Input

4.1 Introduction

Research into modeling and optimizing the profits for material recycling facilities (MRF) has a rich history. The use of network representations of MRFs was introduced by Gutowski et al. [38]. These representations associate a set of parameters with each material separation process, indicating how successful the process is in separating the target materials. Wolf et al. [39, 40, 41] provide a more fundamental description of these representations. A case study for metal separation illustrates how the network representations can be used in practice [40]. Key performance indicators (purity, yield, total throughput) were introduced that can be optimized for given network representations of MRFs [41].

The derived network models were formalized by Testa [42]. Testa also introduced the use of meta-heuristics (in the form of genetic algorithms) for the optimization of the design of MRFs [42]. The study of the optimization of MRFs takes place in two branches [42]. The first branch is the study of specific separation processes, the involved machinery and the chemical properties of materials. The aim of this branch of research is to develop devices for material separation. A detailed overview of existing separation methods and machinery is given in [9, 10].

The second branch is the optimization of the structure of MRFs as carried out in the literature [38 – 42]. The effectiveness of specific separation processes is provided by abstract parameters in the latter branch. Thus, there is a lack of process-specific information in the models in [38 – 42]. In this report, the gap between optimization of MRFs using detailed process-specific information and the large-scale structure of the MRF is bridged. The emphasis is on density-based sorting, as this is the most commonly adopted method in practice according to PolyCE consortium members.

From the process-specific perspective, density separation is studied in depth by Gent et al. [12]. Using density spectra enables the identification of materials that can successfully be separated by density. From the more generic structural perspective, a dynamic programming

(DP) approach to determine the optimal order in which processes with throughput-dependent costs have to be carried out is derived by Sodhi et al. [43]. The insights of Gent et al. [12] and Sodhi et al. [43] are both incorporated in this work.

4.2 Modelling and computation

4.2.1 Density Separation

The experiments described in Chapter 3 provided two classes of proportions. The first is the proportion of density values per material. The second is the proportion of materials per product component. These proportions are treated as the discrete probability density distributions in the remainder. Suppose material m has density ρ with probability $P_m(\rho)$. Suppose further that product p comprise material m with probability $Q_p(m)$. Let v be the vector of masses per product entering the Material Recovery Facility (MRF), such that v_p is the mass of product p. Then the number $E(\rho, m)$, as defined in equation (4.1), is the expected total mass of material m that has density ρ.

$$E(\rho, m) = \sum_p v_p \cdot Q_p(m) \cdot P_m(\rho) \tag{4.1}$$

Note that $E_m := \sum_\rho E(\rho, m)$ is the total mass of mass of material m entering the facility. The vector $E = (E_m)$ is referred to as a stream. Each stream E has (total) mass $M(E) = \sum_m E_m$. Each material m in a stream E has purity $G(m, E)$, as defined in equation (4.2).

$$G(m, E) := \frac{E_m}{M(E)} = \frac{E_m}{\sum_k E_k} \tag{4.2}$$

A density separation step with density value r takes as input a stream E and produces as output two new streams E', E'' such that $E'_m = \sum_{\rho \leq r} E(\rho, m)$ and $E''_m = \sum_{\rho > r} E(\rho, m)$. That is: E' contains all the mass of E that is smaller than or equal to r. Likewise, E'' contains all the mass of E of which the density is larger than r. In particular, $E' + E'' = E$, as shown in Figure 4.1.

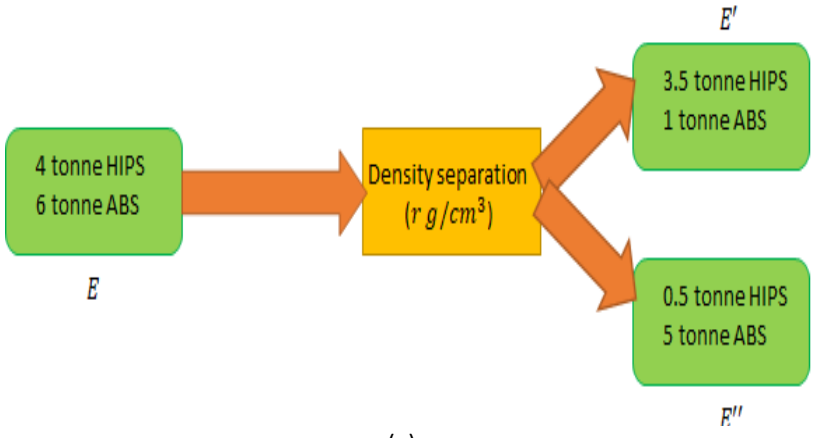

(a)

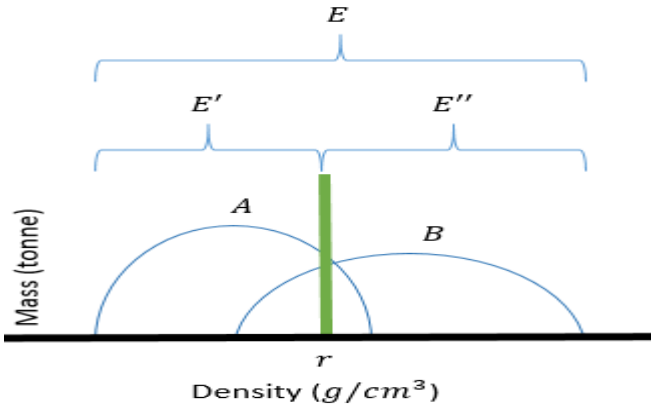

(b)

Figure 4.1. (a) Network representation of a separation operation as introduced in [38, 39]. The green nodes represent a material composition. The yellow node represents a separation operation. (b) Visualization of a separation step on the density spectra weighed by the mass of each product present.

Given an input stream E, the goal is to find a set $R \coloneqq \{r_1, r_2, \dots, r_k\}$ of density values such that once density separation is carried out at all values in R, the resale price of the materials in E is optimized. Assuming n materials have to be separated by at most $n-1$ separation steps, the number of feasible solutions $g(s,n)$ is given in equation (4.3).

$$G(s,n) \coloneqq 1 + \sum_{i=1}^{n-1} \frac{s!}{(s-i)!} \tag{4.3}$$

Here, s denotes the number of density values for a spectrum (i.e. the number of values on the x-axis in Figure 27. (b)). As mentioned in Chapter 3, $s = 48$ in the work reported. One is added to the sum, because not carrying out any separation step is also an option. Intuitively, clustering using graph color features appears to reduce the within-cluster number of materials (since each cluster is developed along a subset of the materials). Regarding computation time, this reasoning unfortunately does not apply in practice, as outliers and contaminations may still be present in a clustered stream. Thus, clustering, while useful for creating higher-purity streams, does not decrease the exponentially-sized solution space. Thus, clustering may drastically improve the possibilities for material separation, while *theoretically* keeping the computation time of the optimal set of separation steps intact.

4.2.2 Near-Infrared Spectroscopy

Using the information outlined in Chapter 3, NIR is more easily modeled in the Bayesian approach. A scheme of a NIR-step is illustrated in Figure 4.2. Note that in this model, the "accuracy" of $\alpha \times 100\%$ of NIR is interpreted in terms of yield.

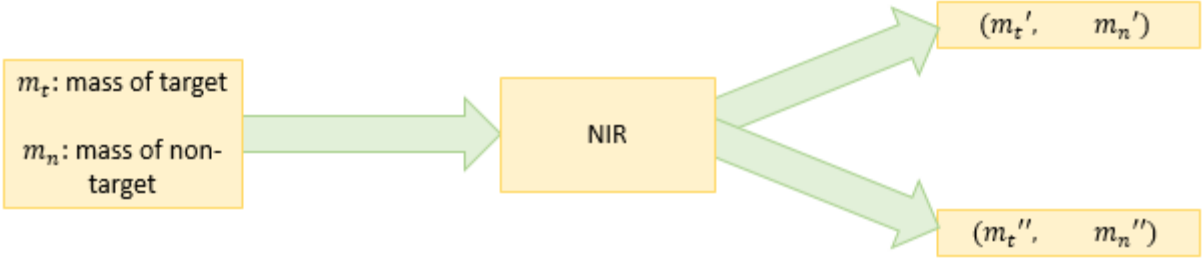

Figure 4.2. NIR separation step, where $m_t = m_t^{'} + m_t{''}$ and $\frac{m_t^{'}}{m_t} = \alpha$

4.2.3 Performance Indicators

In the literature [38 - 41], the most common optimization objectives are increasing purity or yield of some target material. The Pareto front of this trade-off is then subject of study. In the present study, each material is considered a target material. The criterion to be optimized is the sum of resale prices of output streams. A purity of at least 90% is considered sufficient for resale, regardless of the involved material. This threshold was determined in cooperation with industrial partners.

An MRF has two main sources of expenditures. The first are incineration costs for streams failing to reach the targeted purity of 90%. These include costs for transportation, taxes, etc. The second source of expenditures is the operational costs of the separation steps. Density separation incurs a mass-dependent cost through the amortization of machines, energy use and involved labor. These unit prices and costs define the objective function of the optimization problem.

4.2.4 Modeling assumptions

Assumptions 4.1. In addition to the parameter estimates outlined in Chapter 3, the following modeling assumptions are used:

1. Two size reduction steps are always required between input and output materials that can be sold. This is a realistic assumption, since the output materials are sold to compounders in the shape of small flakes (roughly spheres with a radius of $2.5mm$). The size-reduction step in between NIR and density-based sorting is not required if the entire stream obtained after NIR has to be incinerated. Likewise, no size-reduction steps are required if the entire input stream has to be incinerated;
2. There is a size-reduction step between NIR and density-based sorting. That is: NIR necessarily takes place before density-based sorting;
3. In Chapter 3, NIR was described to have an "accuracy" of 80%. This is interpreted in terms of yield;
4. NIR is applied to each target material at most once.

4.2.5 Solution method

This section contains an outline of the method used to optimize the MRFs' profits. The method relies on Simulated Annealing (SA) [44] and Dynamic Programming (DP) [45]. Represent an input stream as a vector, say m, associating with each product component a mass (in tonne) with which that component is present in the stream. Thus, $m_{CRT\ TV}$ represents the mass of CRT TVs in the stream. The first step is to compute an initial feasible solution through a *heuristic* method. Subsequently, this solution is iteratively improved by selecting solutions in its *neighborhood* in a *probabilistic* manner. If some *stopping criterion* is met, this process is terminated. Thus, five concepts have to be designed: the heuristic for the initial solution; a neighborhood function; acceptance probabilities; a stopping criterion (or criteria) and the computation of the objective function value.

4.2.5.1 Heuristic for the initial feasible solution

Density-based sorting

Suppose the input vector m is given. Then the (estimated) mass present per material can be computed using the data from Section 3.3. The normalized density spectra from Section 3.4 can then be scaled by the mass of each material in the stream. This creates spectra with density values along the x-axis and masses along the y-axis. Next, take the maximum of the spectra and smooth it (currently, this is done using an exponential moving average; kernel-density methods or polynomial interpolation are reasonable alternatives). The local minima of the obtained curve now correspond to clear locations where spectra of distinct materials may start to overlap. Furthermore, if a local minimum is close to zero, this indicates that if materials overlap in this point, they can be expected to have a small PAO. This is illustrated in Figure 4.3.

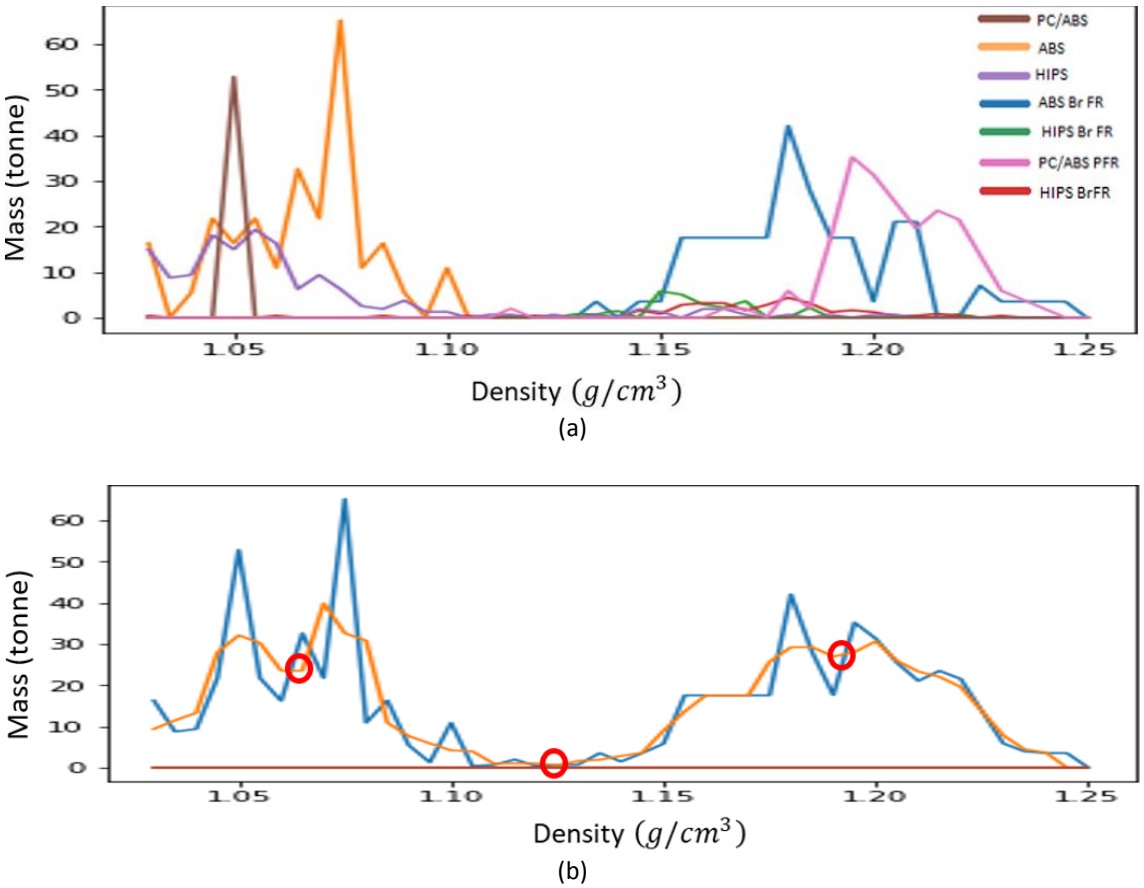

Figure 4.3. Illustration of heuristic (a) Density spectra of hypothetical problem instance (b) maximum of spectra (blue); smoothed maximum (orange) and its local minima (red)

NIR

Algorithm 1 is starting heuristic for determination of NIR target materials.

Algorithm 1: NIR heuristic

Data: Mass-weighed density spectra ("input stream") S; set of materials M with nonzero mass in the input stream; Set N of materials to which NIR is applicable; price threshold τ_p; PAO threshold τ_{PAO}; α: accuracy of NIR sorting

Result: nir: set of target materials for NIR

1 $M^* \leftarrow$ array of materials $M \cap N$ ordered by decreasing value of $mass \times unit\ price$;
2 $\mathcal{M} \leftarrow$ Total mass of input stream;
3 $nir \leftarrow \emptyset$;
4 **for** *each material* $m \in M^*$ **do**
5 Compute the value v_m of the polymer if it were completely isolated (that is: its weight times its unit resale price as a recyclate);
6 **if** $\alpha \cdot v_m > \tau_p \cdot \mathcal{M}$ **then**
7 $P \leftarrow \sum_{m' \in M \setminus \{m\}} PAO'(S, m, m')$;
8 **if** $P > \tau_{PAO}$ **then**
9 $nir \leftarrow nir \cup \{m\}$;
10 $M \leftarrow M \setminus \{m\}$;
11 Reduce the weight of m in the input stream S by $\alpha\%$;
12 Update $\mathcal{M}$ and all PAO' values;
13 **end**
14 **end**
15 **end**
16 **return** nir;

Remark 4.2. *Regarding algorithm 1, note the following:*

1. *Its time complexity is in $O(|M|^3)$, since each iteration requires an updated PAO' table. This complexity is negligible in practice;*
2. *This heuristic takes into account that NIR is more expensive than density separation. Thus, NIR is only taken into account if there are valuable materials that cannot be isolated by density-based sorting methods solely;*
3. *The threshold parameter τ_p should satisfy $\tau_p \geq \frac{1}{2} C_{NIR}$, where C_{NIR} is the processing cost of NIR per tonne. This is apparent in line 6, since NIR is only considered if the profits outweigh the costs. If m is considered and is significantly polluted by m', then m' (very likely, due to line 11) occurs later in M^* than m. As such, it is less valuable. Thus, if the added values of m and m' are both below $\frac{1}{2} C_{NIR}$, then even after both NIR and density-based sorting, the cost of the NIR step is not outweighed by the sum of the resale prices for m and m' (which is less than $2 \times \frac{1}{2} C_{NIR} = C_{NIR}$);*
4. *The reasoning in step 3 can be used to make t_p context-dependent by taking into account the number of "severe" pollutants and their potential;*
5. *Technically, C_{NIR} is dependent on the input stream, hence it can also be updated in step 12 if deemed necessary;*
6. *The accuracy α is interpreted as a yield percentage: $\alpha \times 100\%$ of the target material is recovered from the input stream and $(1 - \alpha) \times 100\%$ remains in the input stream;*

7. *If α is sufficiently large or the masses of each material in the input stream are sufficiently proportionate, then Assumption 4.1 (4) is justified. This is easily seen when considering Algorithm 1, as one step of NIR will likely reduce v_m to below τ_p as well as $PAO'(m, m')$ to below τ_{PAO};*
8. *If the conditions from point (7) are not the case, then Assumption 4.1 (4) could be abandoned. The for-loop of Algorithm 1 (line 3) could then be replaced by a while-loop with stopping criteria stating that the algorithm terminates once all materials fall below one of the thresholds. The set nir can then be replaced by a list that may contain materials several times. A final observation is that the PAO' values used in the heuristic are specific to the spectra in question (as weighted by input masses of product (components) and their polymeric compositions);*
9. *Once data is available for accuracy of NIR for specific target materials, α may become a vector rather than a fixed value. The vector α then contains an efficiency α_m for each $m \in M$;*
10. *If the processing cost of NIR is smaller than the processing cost of density-based sorting, it becomes a better strategy to do most of the separation using NIR. That is: taking a very small value for τ_{PAO};*
11. *Since M' is sorted by potential profit, the algorithm may be considered greedy.*

Aggregation
First apply the NIR heuristic; make sure that the density spectra after this step have reduced weights for materials targeted by NIR; apply the density-based sorting heuristic to the obtained density spectra; apply the further steps of the SA algorithm.

4.2.5.2 Neighborhood function

The neighborhood function is defined through three operations for density-based sorting and two for NIR. For density-based sorting, operations (d1) through (d3) are used.

d1. Adding a density value at which density-based sorting has to be performed;
d2. Removing a density value at which density-based sorting has to be performed;
d3. Moving a density value at which density-based sorting has to be performed.

For NIR, operations n1 and n2 are used.

n1. Remove a target material;
n2. Add a target material.

One operation out of (d1)-(d3) and (n1)-(n2) is selected probabilistically in each iteration. The involved probability distribution over operations is optimized for each problem instance (parameter tuning). Typically, the probability of operation (n1) is very low, as the NIR heuristic seeks out specifically materials that are problematic for density-based sorting. The greedy sorting from Algorithm 1 is used in a softmax distribution to probabilistically make it more likely to select valuable materials for NIR when applying (n2). An acceptance probability decreasing with the computational temperature manages the selection of successor solutions.

4.2.5.3 Acceptance probability and stopping criterion

The acceptance probability is an important aspect of SA, as it prevents terminating in local minima and manages the trade-off between exploration and exploitation of neighborhood information. The acceptance probability can be interpreted as the proportion of neighboring

solutions accepted, even though their objective value is below that of the currently best known solution. The probability is initialized close to one – fostering the ability to explore. Once good solutions are discovered, the probability is lowered every several iterations, to facilitate the exploitation of the currently best solutions. The decrements of the probability are dependent on the degree of improvement since the last update. An additional variable, referred to as the temperature, is initialized and updated in a comparable manner. The algorithm is terminated once the temperature is sufficiently small.

4.2.5.4 Computation of objective function value

For a given solution, the objective value has to be computed. The purities and yields per stream are easily computed and subsequently, the yield can be multiplied by the input mass to obtain the output mass. If the purity of the involved material exceeds the 90% threshold, then the output mass can simply be multiplied by the unit price of the recyclate. Likewise, the energy recovery (incineration) costs of fractions deemed not pure enough are easily computed by multiplying the involved mass by the unit energy recovery costs.

Processing costs are less easily computed, as the order in which separation steps (NIR or density-based sorting) are carried out impact the mass left to be separated. This results in a recursive problem structure. Sodhi et al. [43] propose a dynamic programming (DP) approach to solve the problem. This DP method is characterized by recurrence relation (4.4). This relation takes into consideration only the sum of masses. As a linear processing cost function is used, the sum of masses can be computed first and subsequently multiplied by the unit processing cost. As a remark, expression (4.4) is paraphrased and presented in a more intuitive manner than in [43].

$$\begin{cases} c(i,1) = 0 \\ c(i,j) = \sum_{k=i}^{i+j} M_k + \min_{\mathrm{r}=1,2,\ldots,\mathrm{j}-1}\{c(i,i+r) + c(i+r+1,j \end{cases} \quad (4.4)$$

In recurrence relation (4.4), $c(i,j)$ denotes the cost of carrying out a DBS step that affects the regions $i, i+1, \ldots, i+j$ that are not yet (but will be) separated. Variable M_k denotes the mass of region k. Thus, the summation in the latter equation indeed models that a separation step has as processing cost (a linear function of) all the surrounding masses yet to be separated. The minimum taken is due to the fact that carrying out some separation step r entails splitting up the problem into two new smaller problems. The minimal value of these two subproblems therefore determines which value of r is optimal, exemplifying the recursive nature of the problem. The first equation in recurrence relation (4.4) terminates the recursive calls, as no processing cost is incurred if the region under consideration is already separated. Regarding the method from [43], the following statements are presented without proof.

Proposition 4.3. The method in [43] has a running time that is exponential in the number of masses to be separated, even when storing solutions of overlapping subproblems in memory.

Proposition 4.4. The problem of minimizing the operation costs is in complexity class P.

Finally, the most commonly adopted method in practice (according to discussions with PolyCE partners), recursively separating materials at the separation value closest to the total center of mass, was analyzed, resulting in Proposition 4.5. The proof of this proposition is also omitted, although it is a lot more straight-forward (see [46], chapter 3 for some background on approximation guarantees).

Proposition 4.5. The method of separating a waste stream recursively by the separation value closest to the center of mass of the stream has a worst-case-ratio (WCR) of at least $4/3$.

The proof of Proposition 4.4 relies on the similarity between the problem in question and the minimum-cost maximum-flow problem (see [45, 47]). The proof of Proposition 4.3 relies on a combinatorial method to count the number of unique solutions. This method also provided an (exponential time) algorithm that outperforms both the method described in [43] and the polynomial time method in practice. This new method is referred to as the vectorized method or vectorization (in analogy to popular jargon in python programming, where replacing iteration using linear algebra is considered a best practice). Figure 4.4 contains a comparison of the computation times of the DP and the vectorized approaches for 100 random experiments for each of the problem sizes in $\{2,3,\dots,10\}$. Recall that this subproblem has to be solved for every candidate solution in the SA algorithm. Hence, the computational time is of key importance.

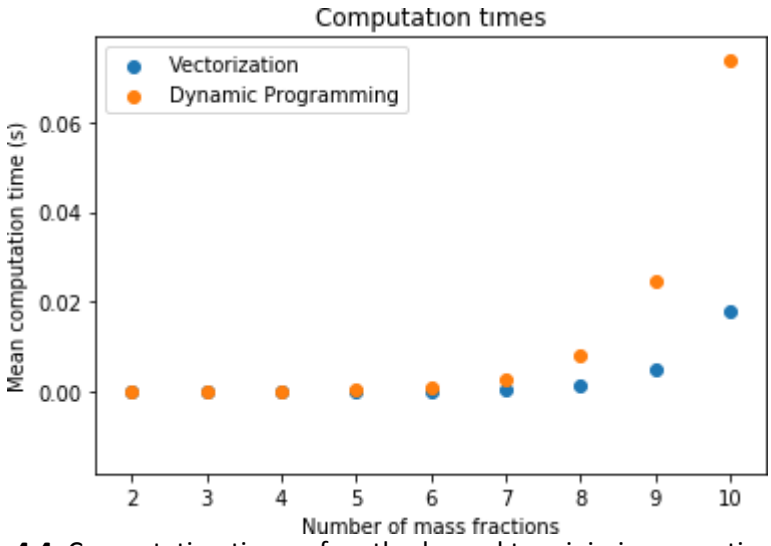

Figure 4.4. Computation times of methods used to minimize operation costs

5 Identification of Promising Potential Clusters

5.1 Introduction and approach

In this chapter, the gathered data are used to develop clustering strategies for components of products from WEEE. To this end, the following steps are taken:

1. **Feature Engineering.** To optimally use the existing data, new features (that is: attributes/variables) are introduced. In particular, a matrix representing the applicability of density separation is derived. Using this feature, product components are not classified by their main polymeric constituents. Instead, they are partitioned into classes of easily separable materials. This feature engineering task requires some basic concepts from the field of graph theory [47]. These concepts are briefly introduced to keep the report self-explanatory. The developed methodology is then also generalized to incorporate plastic miscibility. Examples of how to incorporate multiple material properties using the graph theoretic approach are thereby provided.

   Various ways to incorporate multiple material properties using the graph theoretic approach are then illustrated. The methodology developed is subsequently applied to material miscibility.
2. **Outlier detection.** To prevent peculiar data points from corrupting otherwise straight-forward clustering strategies, outliers are detected and removed from the data. In particular, use is made of an isolation forest.
3. **Clustering.** Finally, clusters are formed by inspection and by a statistical clustering method. The parameters of these methods are optimized so that the method is adequately applied to the data. The method is applied to the complete data set. To deal with the shortcomings in the data, a more detailed case study is carried out in Chapter 6.

Throughout the remainder of this report, computational experiments are carried out on an Intel® Xeon® CPU E3-1270 v5@ 3.60 GHz, x64-based processor with 32.0 GB of RAM. Algorithm implementations used for this purpose were developed in Python™ 3.6.

5.2 Feature Engineering

5.2.1 Preliminaries

The graph coloring problem is briefly introduced in this section. For a more thorough account of graph theory, the reader is referred to [45, 47].

Definition 5.1. Let $G = (V, E)$ be a simple graph. Let C be a sufficiently large set of colors. A **vertex coloring** of G is a function $f: V \to C$ such that $f(u) \neq f(v)$ whenever $\{u, v\} \in E$.

If f is a vertex coloring on G and $|Im(f)| = k$, we will say that f uses k colors or, alternatively, that f is a k-coloring of G. The graph coloring problem can now be introduced.

Problem 5.2. (Graph coloring problem)
Given is a simple graph $G = (V, E)$. Find a vertex coloring f using the smallest number of colors possible.

Example 5.3. The map

$$f(x) = \begin{cases} 1, & if\ x \in \{A, B\} \\ 2, & if\ x \in \{C, D\} \end{cases}$$

Is a 2-coloring of the graph depicted in Figure 5.1.

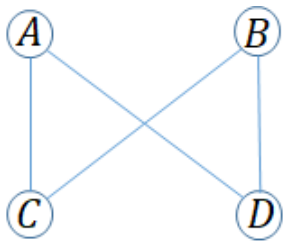

Figure 5.1. Example of a graph

The complement of a graph G is denoted by G'. Proposition 5.5 outlines an interpretation of a vertex coloring on the graph's complement. The proposition is easily verified, for instance by using duality in integer programming formulations (see, e.g., [46]).

Definition 5.4. Let $G = (V, E)$ be a simple graph. A **clique** in G is a complete subgraph of G.

Proposition 5.5. Let $G = (V, E)$ be a simple graph. Suppose that f is a vertex coloring in G with the smallest possible number of colors. Then f is a decomposition of G' into cliques with the smallest possible number of cliques.

5.2.2 Features for density separation

In this section, a method is designed to construct features that incorporate the effectiveness of a material separation process. The method is modular in nature. Nonetheless, due to the restrictions on the available data and for the sake of readability, the method is illustrated using DBS. In Chapter 3, it was illustrated how the efficiency of density-based sorting when applied to two distinct polymers can be quantified. The Partial Area of Overlap (PAO) was introduced for this purpose (cf.Figure 3.15 and Table 3.5). In the remainder of this section, the PAO concept is used to generate features to represent density-based sorting in the context of statistical clustering algorithms.

5.2.2.1 Constructing a separation graph

Suppose $\tau \in [0,1]$ is a threshold parameter, such that DBS is considered suitable for materials i and j if, and only if, $PAO(i,j) \leq \tau$. For a set S of materials and parameter τ, the *density graph* $Dens_\tau(S)$ is implicitly defined in expression (5.1).

$$\begin{cases} Dens_\tau(S) \coloneqq (S, E_\tau(S)) \\ \{i,j\} \in E_\tau(S) \Leftrightarrow PAO(i,j) \leq \tau \end{cases} \tag{5.1}$$

A small example outlining the relation between density spectra and their density graph is included in Figure 5.2.

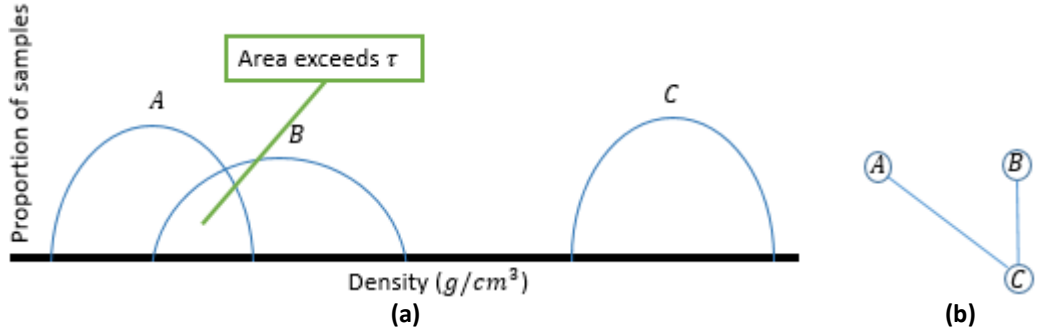

Figure 5.2. (a). Normalized density spectra for hypothetical materials A, B and C. **(b).** Corresponding density graph

5.2.2.2 Decomposing the density graph

Consider the subgraph $H_\tau(T)$ of $Dens_\tau(S)$ induced by some set $T \subseteq S$ of materials. Note that trivially, H_τ is complete if, and only if, $PAO(i,j) \leq \tau$ for all $i,j \in T$. This is formalized in Observation 6.6.

Observation 5.6. Let τ be given. Let $H_\tau(T)$ be a subgraph of $Dens_\tau(S)$ induced by a set $T \subseteq S$. Then DBS can be applied to separate all the materials in T if, and only if, $H_\tau(T)$ is complete.

A direct consequence of Observation 5.6 is that if $Dens_\tau(S)$ is decomposed into cliques, then the materials in each of these cliques can be liberated using only DBS. By Proposition 5.5, an optimal manner of grouping together materials such that DBS is applicable is therefore a vertex coloring on the complement $Dens'_\tau(S)$ of $Dens_\tau(S)$ that uses the smallest possible number of colors. In Figure 5.3, two possible 2-colorings of the complement of the graph from Figure 5.4(b) are depicted. Note that these indeed correspond to decompositions of the original graph into two cliques.

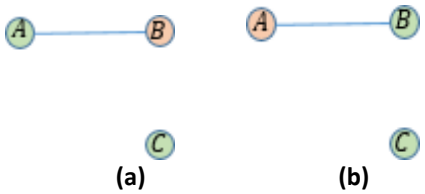

Figure 5.3. 2-colorings

In simple terms, whenever there is an edge in the graph between the vertices of two polymers, these polymers can be separated using density-based methods. The aim is to decompose the graph into subgraphs such that there is an edge between any pair of vertices in any subgraph (in the example in Figure 5.4, such a decomposition would be {{A,C},{B}}; {{A},{B,C}} or {{A},{B},{C}}). The decomposition satisfying this property assigns each polymer to a class in which all polymers can be isolated using density-based sorting. Such a decomposition is most efficient if it has as few subgraphs as possible (as this requires the least effort for clustering).

5.2.2.3 Converting colorings to features

Suppose the graph $Dens_\tau(S)$ was obtained for material set S and threshold τ. Suppose that $f: S \to C$ is a $|C|$-coloring of complement $Dens_\tau'(S)$. Compute the inverse relation $f^{-1} \subseteq C \times S$. Note that $f^{-1}(c), c \in C$ is a non-empty set of materials, not a unique material. For instance, in the graph from Figure 12(b), $f^{-1}(green) = \{B, C\}$.

Using the data regarding polymer compositions of product components, features can be created for each color. Let P be a product component. For each material $s \in S$, let P_s denote the proportion of material s present in component P. For each color $c \in C$, we can now compute the degree $dens_c(P)$ to which product P belongs to color c in a coloring of the complement of a density graph through equation (5.2).

$$dens_c(P) := \sum_{s \in f^{-1}(c)} P_s \tag{5.2}$$

In this manner, if the complement of the density graph is colored using k colors, k new features

$$dens_1, dens_2, \dots, dens_k$$

are constructed. These features express how well product components can be separated using DBS when treated jointly.

5.2.2.4 Example: density features using realistic data

The approach from Sections 5.3.1 through 5.3.4 was applied to the data outlined in Sections 3.3 and 3.4. Figure 5.4 depicts the density graph of the realistic data (see Table 5) for $\tau = 0.04$ and its complement. Table 5.1 contains the inverse relation of a minimal graph coloring of the complement of this density graph.

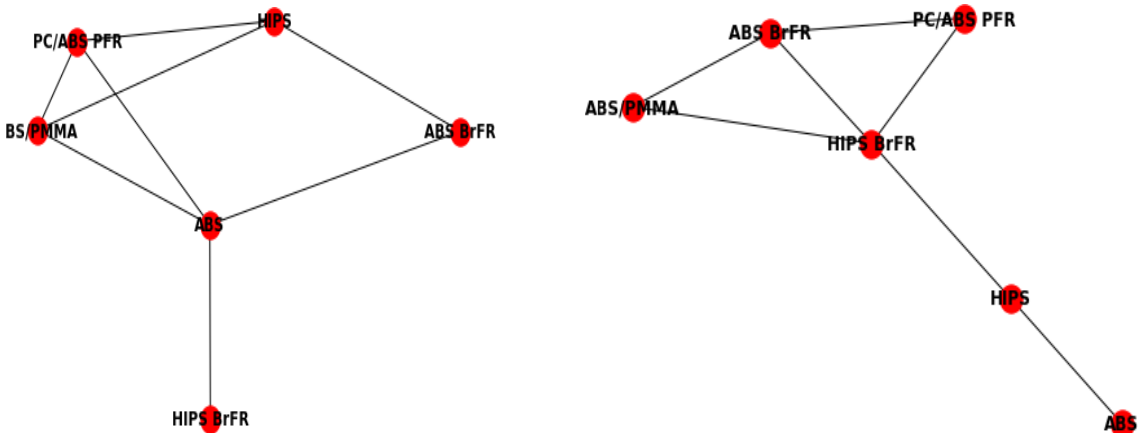

(a) **(b)**

Figure 5.4. Density graphs for $\tau = 0.04$. (a). Density graph constructed using available data (b). Complement of density graph

Color	Materials
1	HIPS BrFR; ABS
2	HIPS; ABS BrFR
3	ABS/PMMA; PC/ABS PFR

Table 5.1. Decomposition of density graph for $\tau = 0.04$

The number of edges in a density graph $Dens_\tau$ increases with τ. As a consequence, the number of edges in $Dens_\tau'$ decreases as τ increases. Thus, as τ increases, fewer colors are

required in a coloring of $Dens_\tau$. This results in fewer, larger cliques. Figure 5.5 and Table 5.2 illustrate this, as τ is placed at 0.3. Obviously, the lower the value of τ is, the more reliable DBS is within cliques. The optimal value of τ is therefore domain-specific information.

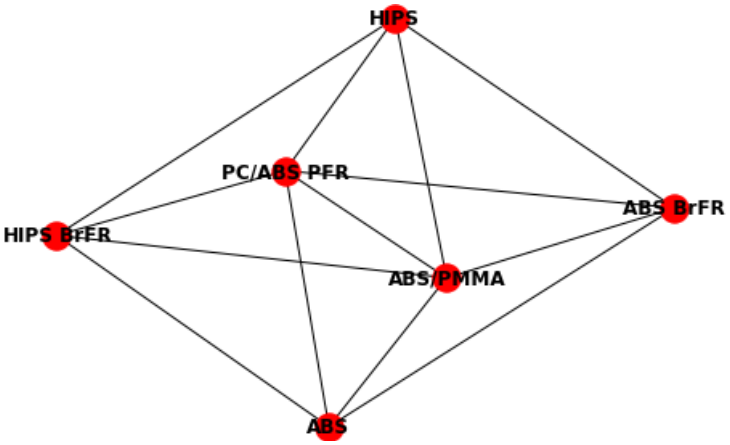

Figure 5.5. Density graph for $\tau = 0.3$

Color	Materials
1	ABS BrFR; ABS; ABS/PMMA; PC/ABS PFR
2	HIPS; HIPS BrFR

Table 5.2. Decomposition of density graph for $\tau = 0.3$

5.2.3 Combining features obtained from graph colorings

Whenever an efficiency table is available for a separation process, the steps outlined in Sections 4.2.2.2 through 4.2.2.4 can be applied. In this section, ways to combine information regarding distinct sorting processes are discussed. When dealing with multiple separation processes x, y, their thresholds are denoted by τ_x, τ_y, respectively.

Suppose efficiency tables are available for two processes x, y. The most straight-forward approach for combining the information of these processes is to derive separate color-features for both of them, giving $k_1 + k_2$ new features $x_1, \dots, x_{k_1}; y_1, \dots, y_{k_2}$. An advantage of this approach is the transparency after clustering. Suppose m products $P^1, P^2, \dots, P^m$ are clustered together. Suppose further that inspection of the features shows that these products were clustered together, because all of them have large values in feature y_i for some i. Then it is immediately apparent that this cluster should be separated using technology y. A disadvantage is that products may be clustered together due to poor or average separability of the involved materials for all technologies.

A different approach to combining sorting techniques when deriving features is the following. Suppose that materials i and j cannot be separated adequately by process x, but can be separated by process y. Rather than deriving separate features for x and y, note that it suffices to know whether i and j can be separated by x *or* y. Thus, the graphs $G_x = (V_x, E_x)$ and $G_y = (V_y, E_y)$ of processes x and y, respectively, can be constructed. Subsequently, the graph $G_{x \vee y} = (V_x \cup V_y, E_x \cup E_y)$ and its derived features describe how well the materials can be separated by at least one of the processes. This graph can be efficiently computed by taking

element-wise maxima in the adjacency matrices G_x and G_y. An advantage of this approach is that it models how the availability of more sorting technologies is less constraining from a clustering point of view. A disadvantage is the lack of transparency as previously described. In particular, the fact that the features combine distinct processes makes them abstract by nature.

To illustrate the latter approach, the density graph obtained in Section 4.2.2 is combined with the information regarding polymer miscibility from Section 3.5. So far, the feature engineering techniques outlined concerned separation processes. Note that miscibility may be treated in the same manner, the only difference being that materials are blended instead of separated. Thus, we may treat Figure 3.17 as an efficiency table. The threshold t_{misc} is chosen so that only the value "G" in Figure 3.17 is considered sufficiently miscible. As this is a categorical variable, this threshold is denoted by $\tau_{misc} = 'G'$. The complement of the obtained graph G_{misc} and the complement of $G_{misc \vee dens}$ are depicted in Figure 5.6. A decomposition for $G_{misc \vee dens}$ is provided in Table 5.3.

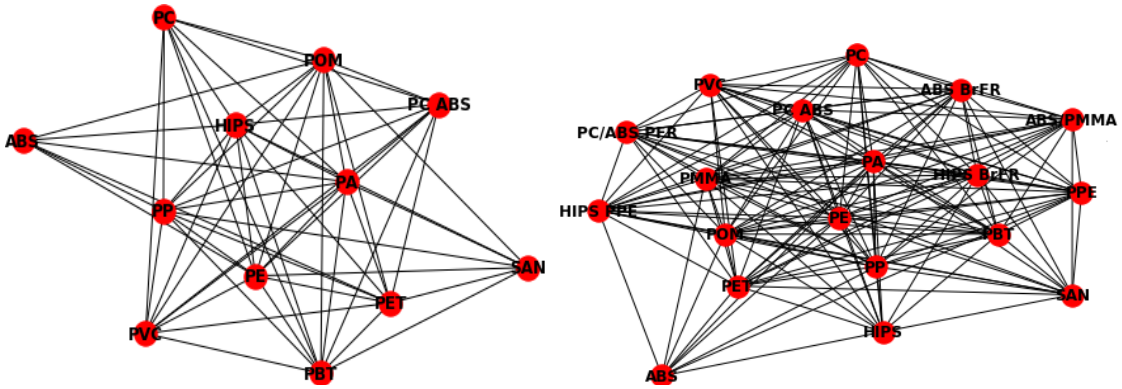

(a) (b)

Figure 5.6. (a). Complement of graph of material miscibility, $\tau_{misc} = 'G'$ (b). Complement of union of miscibility graph and density graph with $\tau_{dens} = 0.04, \tau_{misc} = 'G'$

Color	Materials
0	POM
1	PE
2	PP
3	PA
4	HIPS BrFR; ABS
5	PET, PC
6	ABS BrFR; HIPS
7	PBT
8	PMMA; PVC; SAN
9	PC/ABS
10	PPE; HIPS/PPE
11	ABS/PMMA; PC/ABS PFR

Table 5.3. Decomposition of $G_{misc \vee dens}$ for $\tau_{dens} = 0.04, \tau_{misc} = 'G'$

5.3 Outlier detection

After generating the features using the outlined methods, outliers were detected using isolation forests [48]. In this section, the method is briefly described. For a more formal account, the reader is referred to [48]. Given a data set with numerical attributes, an isolation tree is a tree constructed according to the following steps:

1. Randomly choose an attribute;
2. Introduce a branch for a randomly chosen value in its range;
3. Continue with the next attribute;
4. For each sequence of attribute values (each branch in the tree), there is a number of observations that take on all these specific values. Stop building when there is only one observation in the branch.

The more similar an observation is to a collection of other observations, the harder it is to isolate by bifurcating along attributes. Thus, observations isolated by short branches may be considered outliers. Outliers are defined as observations with sufficiently short paths in the tree. The structure of an isolation tree is depicted in Figure 5.7.

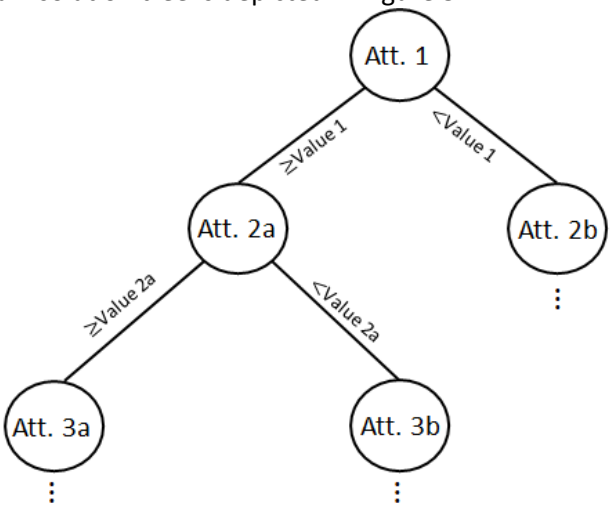

Figure 5.7. Illustration of an isolation tree

An isolation forest is a collection of isolation trees constructed on the same data set. Since the order of attributes and the values in their ranges are chosen randomly, trees in an isolation forest are distinct. The average length from the root of a tree to a specific observation in each of the trees is now a more robust measure of the observation's likeness to other observations.

5.4 Clustering and parameter tuning

5.4.1 Clustering by inspection

5.4.1.1 Introduction

Proper data visualization provides a lot of insight into potential cluster formation. In this section, clusters are derived based on visual information. First, features are generated using the techniques outlined in Section 5.2. Patterns are then observed in a representation of the data as a *heat map*. In this case, such maps are grids with product component categories along the y-axis and features along the x-axis. Each cell in the grid is colored. The darker the shade of grid (x, y), the higher the value of feature x in component y.

Remark. The ease of inspecting the data visually results to an extent from the lack of data. Various product components in the data were measured with very small sample sizes. This makes the data regarding these products perhaps unrealistically homogeneous. This could (partially) explain the ease of the visual methods

Figure 5.8 is a heat-map obtained when combining information regarding ease of density-based sorting with miscibility. Feat_0, Feat_1 and Feat_2 are names designated to the derived features. ABS/PMMA forms its own category, as it occurred as a singleton color class. Furthermore, its rare use in the studied product components is apparent in both Figure 5.8 and Figure 3.9.

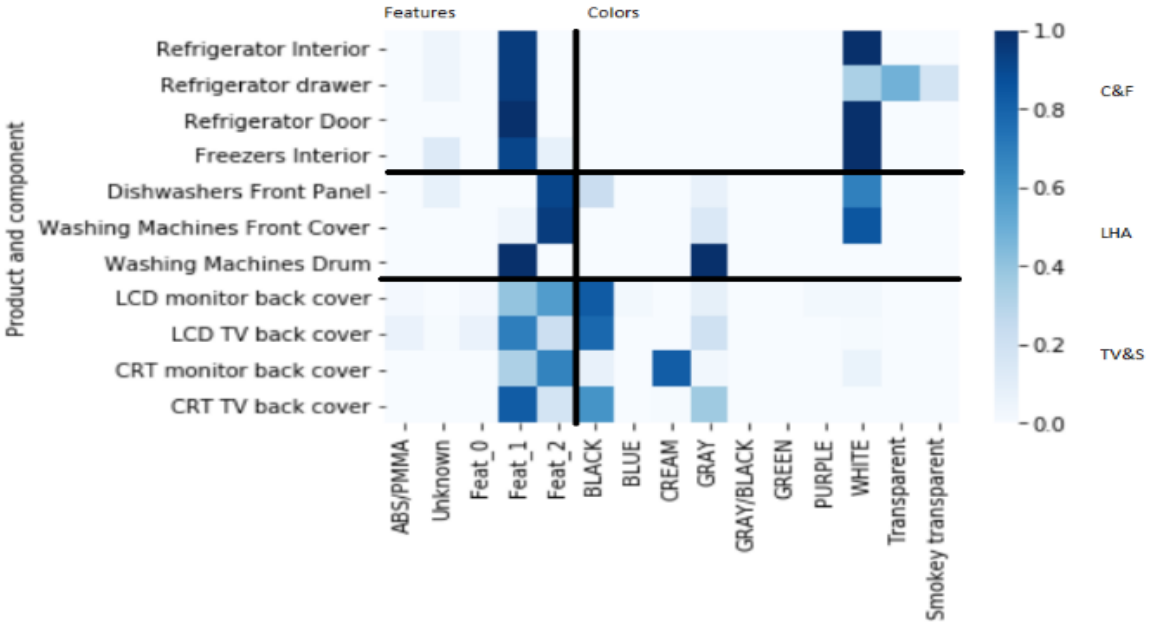

Figure 5.8. Heat-map of features for data regarding disks

The pivotal role played by the feature engineering step is evident when comparing Figures 3.9 and 5.8. Particularly, for the TV&S product components. In Figure 3.9, the composition of CRT TV back covers appears to be highly complex. In Figure 5.8, this composition is narrowed down almost exclusively to one feature (feat_1). This indicates that while a stream of CRT TV back covers may contain many distinct polymers, they can all easily be separated using density-based methods. Furthermore, contaminations of remaining traces of non-target polymers are no huge threat to the output polymer, as they are easily blended without significantly impacting the overall physical properties.

Figure 5.8 can easily be used for clustering based on inspection. For instance, the figure clearly indicates that LCD TV back covers and CRT TV back covers have similar compositions in terms of generated features as well as colors. Likewise,, dishwasher front panels and washing machine front covers have very similar compositions both in terms of density/miscibility features and colors. The same does not hold for the two categories of monitor back covers: their composition in terms of features is more diverse and their color features are different.

5.4.2 Clustering using k-means

5.4.2.1 Introduction

In the light of the remark, the inclusion of more data points may make visual inspection insufficient when defining clusters. A statistical clustering method is then a promising alternative to derive meaningful clusters. The k-means clustering method [49] is particularly interesting for the problem of interest, because all of its attributes take on continuous numerical values. The means of clusters therefore have clear physical interpretations and can be computed using standard distance measures. Furthermore, the sum of squared errors (SSE) can be computed and serve as an indicator of the performance of the method [49].

A brief description of the k-means algorithm using the $MixSep$-variables introduced previously is now provided. An accessible and more comprehensive introduction can be found in [49]. Suppose the data set consists of product components that are composed of 12 $MixSep$ attributes. Interpret the Cartesian product, say D, of the ranges of these attributes as a subset of the 12-dimensional Euclidean space $\mathbb{R}^{12}$. Each data point can then be associated with a point in this space. The distance $d(x, x^{'})$ between two points $x, x' \in \mathbb{R}^{12}$ can be computed using the Pythagorean Theorem (Euclidean distance) with expression (5.3).

$$d(x, x') \coloneqq \sqrt{\sum_{i=1}^{12} \left(x_i - x_i^{'}\right)^2} \tag{5.3}$$

The k-means algorithm takes as input the data set and a positive integer k. It then clusters the data points according to the following steps (where X is the set of data points and μ_{M_i} denotes the mean of cluster M_i):

1. Choose k points $m_1, m_2, \dots, m_k$ in D randomly;
2. Initialize k empty clusters $M_1, \dots, M_k$;
3. Assign each data point $x \in X$ to cluster M_{l^*}, where $l^* \coloneqq argmin_l\, d(x, m_l)$;
4. Put $m_i = \mu_{M_i}$ for all i;
5. Repeat steps 3 and 4 until the means remain unaltered.

5.4.2.2 Evaluation of clustering policies

For each value of k, the optimization routine can be applied to each of the k obtained clusters. Taking the aggregate over all clusters, the overall profit for each clustering policy can be computed. In this manner, the profits of clustering are determined for each number of clusters in $\{1,2, \dots, 11\}$ is determined. These profis are depicted in Figure 5.9. The optimal number of clusters is then chosen (it is the number of clusters after which adding more clusters does not significantly increase the profits; see the “elbow method” in [49]). In the example in Figure 5.9, this number is clearly four. The main sources of separation cost that are throughput-dependent are indiscriminant of the number of clusters (cf. Section 3.4.5). An economic evaluation of the effectiveness of clustering should therefore predominantly focus on the return on the investment with respect to the one-time costs of €30000 per cluster and the annual €500 maintenance costs. In such an evaluation, the annual throughput of an MRF can

be taken into account. This allows for the financial evaluation of the different clustering sizes, where (in the case of Figure 5.9) four can serve as an upperbound.

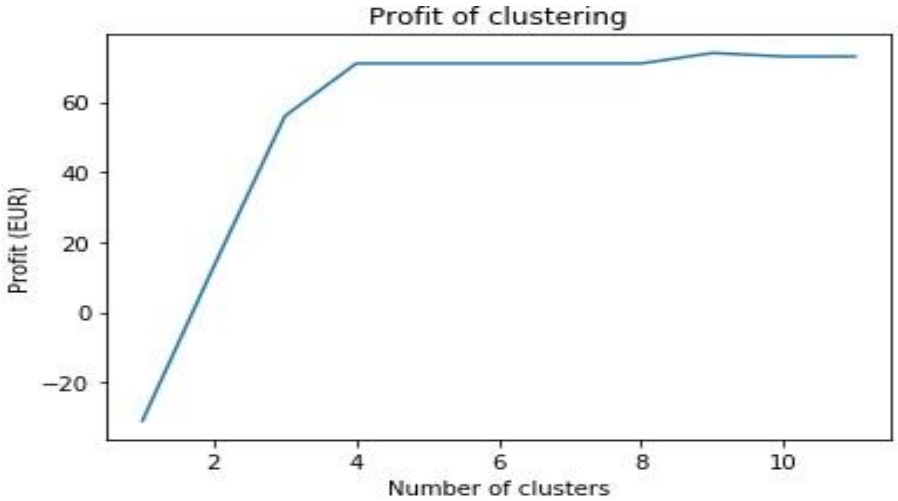

Figure 5.9. Profit of clustering per number of clusters per tonne

5.4.2.3 Clustering results

The clustering algorithm was applied to the full data set of disk measurement results. Features were constructed cmbining ease of density separation with plastic miscibility, resulting in ten features, labeled $MixSep_1, \dots, MixSep_{10}$. Three of these features ($MixSep_4, MixSep_6, MixSep_{10}$) accounted for over 95% of the total variability. As such, three main clusters can be identified, each having one of these three features as their main constituent. The resulting clusters are provided in Table 5.4.

$MixSep_6$	$MixSep_4$	$MixSep_{10}$
Dishwashers front panel	Washing machine tank	Hair dryers main body
Washing machines front cover	Refrigerator door	Laptops bottom cover
Washing machines dispenser drawer	Refrigerator interior	Laptops maintenance cover
Washing dryers front cover	Refrigerator cabinet	Laptops display frame
Household heating side	Freezer interior	Laptops top cover
Food equipment container	Hot water equipment water box	Laptops back cover
Hot water equipment back cover	Printers base cover	Game consoles top cover
Hot water equipment front	Printers side	Cooled dispensers front panel
Vacuum cleaners back cover	Audio equipment base	Mobile phones back cover
Vacuum cleaners removable drawer	Audio equipment side	LCD TVs front cover
Telecom top cover	Speakers side	
LED TV enclosure	CRT TV back cover	
LED TV stand	LED TV back housing	
	LED TV front frame	
	Special lamps side	

Table 5.4. Obtained clusters, characterized by their main feature

6 Demonstrator Cases

6.1 Motivation

To evaluate the potential of product clustering, three demonstrator cases were selected. Potential clusters and target polymers were determined through the use of Tables 3.2 and 3.3 as well as discussions with PolyCE partners. The obtained clusters and targets are stratified by three WEEE categories (C&F; LHA and SHA). Internal discussion indicated that these three streams are typically already collected separately and undergo distinct processing, so that clustering strategies for each category are relatively easily implemented in practice. Throughout this chapter, it is assumed that the efficiency of NIR (the parameter α) is 90% (see Assumptions 4.1).

6.1.1 Cooling and Freezing Equipment (C&F)

Table 3.2 shows that the refrigerators are the main constituent (in mass percentage) of the C&F stream with $93\ wt\%$. In PolyCE work packages 4 and 7, the possibility to obtain food-grade plastic recyclates from end-of-life refrigerators is investigated. The stream of (household) refrigerators garners special attention in these investigations, as these products designed specifically to come into contact with food. Discussion regarding food-grade recycling focused mostly on refrigerator cabinets (drawers). Drawers have the advantage that they are easily removed from refrigerators. Furthermore, plastics in other components of refrigerators are typically glued, making them unsuitable for food-grade applications.

Despite these discussions, food-grade qualification requirements (an output of work package 4) are still lacking. Furthermore, insufficient technology is currently available at KU Leuven to analyze samples with the degree of sophistication that food-grade testing would require. The analysis of plastic samples from refrigerators (as a whole) and refrigerator cabinets in isolation may still lead to interesting conclusions. This is due to the possibly higher homogeneity in terms of polymeric composition for cabinets as well as the ease of disassembly. Furthermore, the typically light color of the cabinets makes them suitable for optical sorting technologies and easy to equip with the color desired by the OEM.

6.1.2 Large Household Appliances (LHA)

Table 3.2 indicates that washing machines are the main constituent of the LHA stream (with $72wt\%$). Discussion with PolyCE partners (Whirlpool; ECODOM) indicated that the drums of washing machines are likely to contain a significantly larger and less polluted fraction of (filled) PP. Consequentially, investing in removing the drums prior to treatment may contribute to higher PP recycling rates.

6.1.3 Small Household Appliances (SHA)

The SHA WEEE category is particularly troublesome due to its complexity. To determine the composition of the overall SHA stream, the results documented in Table 3.3 serve as the main reference (further corroborated by [22]). Aggregating data from this table, one may assume

that the mass percentage of domestic printers constitute $7.8\ wt\%$ of the total SHA WEEE category. For vacuum cleaners ans coffee machines, these percentages are $3.7\ wt\%$ and $2.9\ wt\%$, respectively. Due to the diversity of SHA, no other products were present in ECODOM's trials in weight percentages exceeding $2.9\ wt\%$. Currently, the SHA category is deemed too complex for clustering. A clustering policy targeted towards the three mentioned most prevalent SHA products therefore has the potential to improve the status quo considerably.

6.2 Experimental Results: Material composition

Data in this chapter rely on the results presented in Chapter 3 as well as on [7], Deliverable 3.1 of the PolyCE project.

6.2.1 Cooling and Freezing Equipment (C&F)

6.2.1.1 Results

Figure 6.1 depicts the polymeric composition of the full C&F stream as reported in [7]. Figure 6.2 shows the polymeric composition of the FTIR sampling campaigns carried out at KU Leuven on batches. Color distributions based on computer vision are included in Figure 6.3. It is important to note here that transparent colors are hard to identify by computer vision. Blue and green colors may in fact be observations of the underlying surface through transparent flakes.

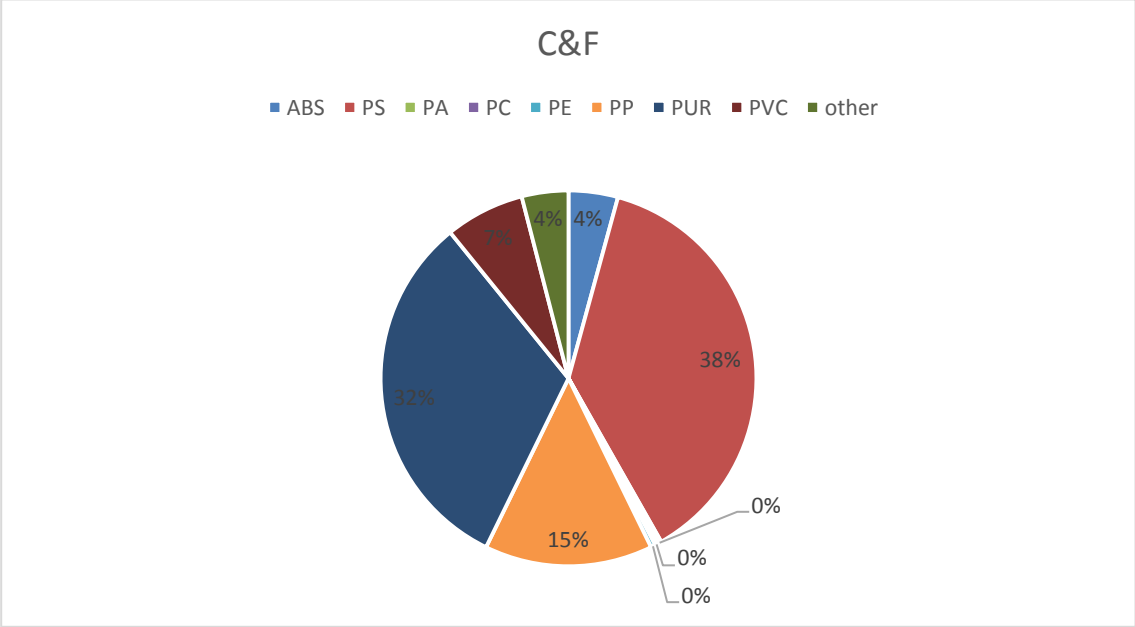

Figure 6.1. Polymeric composition of the cooling and freezing stream

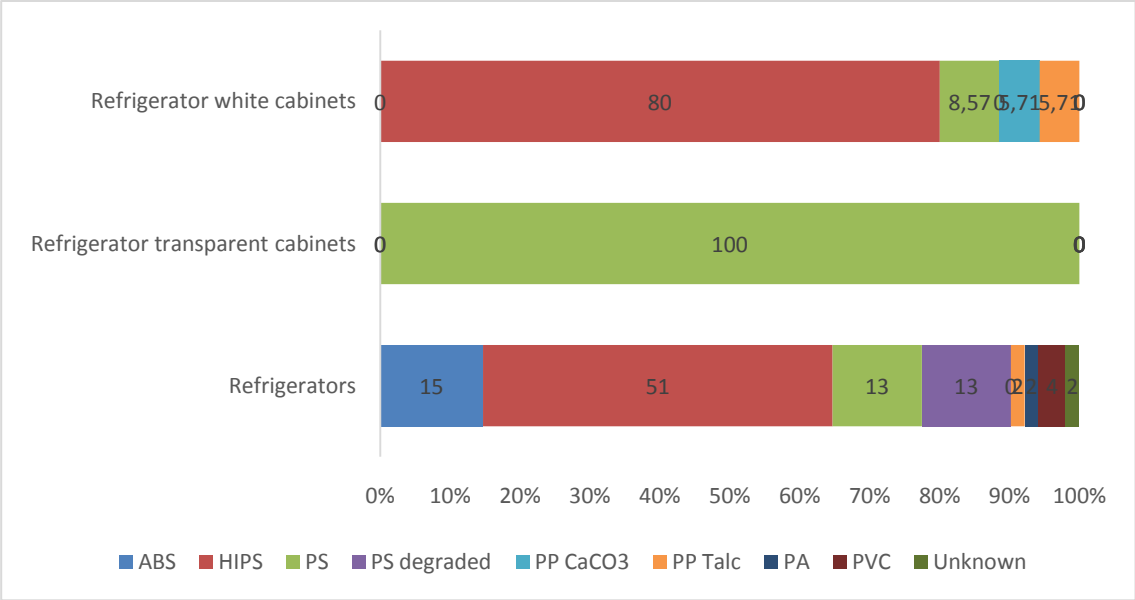

Figure 6.2. Polymeric composition of the three substreams: white cabinets; transparent cabinets; refrigerators (as a whole)

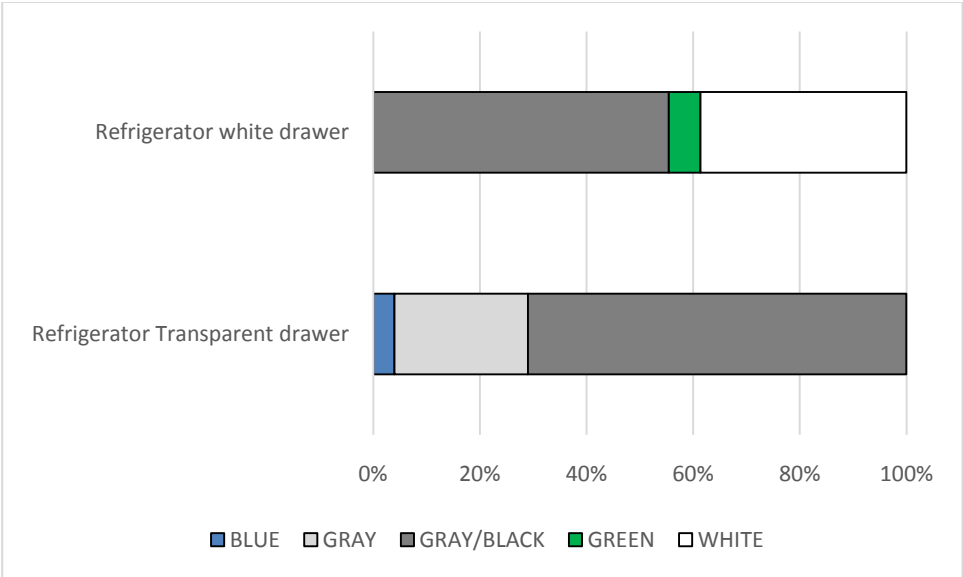

Figure 6.3. Color distribution of refrigerator cabinets

6.2.1.2 Discussion

As expected, the polymeric distributions of refrigerator cabinets are more homogenous than the plastics of refrigerators when treated as a whole. It is worth pointing out that there is a significant difference between the compositions of white cabinets (predominantly HIPS) and transparent cabinets (predominantly PS). Roughly 50% of the PS found in refrigerators was observed to be degraded beyond acceptable standards. This was not reflected in the refrigerator cabinet analysis results. The difference in composition between the total C&F stream and the refrigerator stream is surprising, given that the latter is the main constituent of the former.

Discussion with PolyCE partners indicated that transparent recyclates can be used in white final applications. The substantial presence of (dark) grey colors in the refrigerator cabinet clusters, however, makes their output unsuitable for application in white products. Discussion with PolyCE partners indicated that transparent recyclates can be used in white applications. The substantial presence of (dark) grey colors in the refrigerator cabinet clusters, however, makes their output unsuitable for application in white products.

In conclusion, refrigerator cabinets are indeed more homogeneous in polymeric composition than entire refrigerators. The presence of dark flakes in the sample indicates that plastic recyclates from drawers are unsuitable for resale as white plastics.

6.2.2 Large Household Appliances (LHA)

6.2.2.1 Results

Figure 6.4 contains the polymeric compositions of washing machines and washing machine drums.

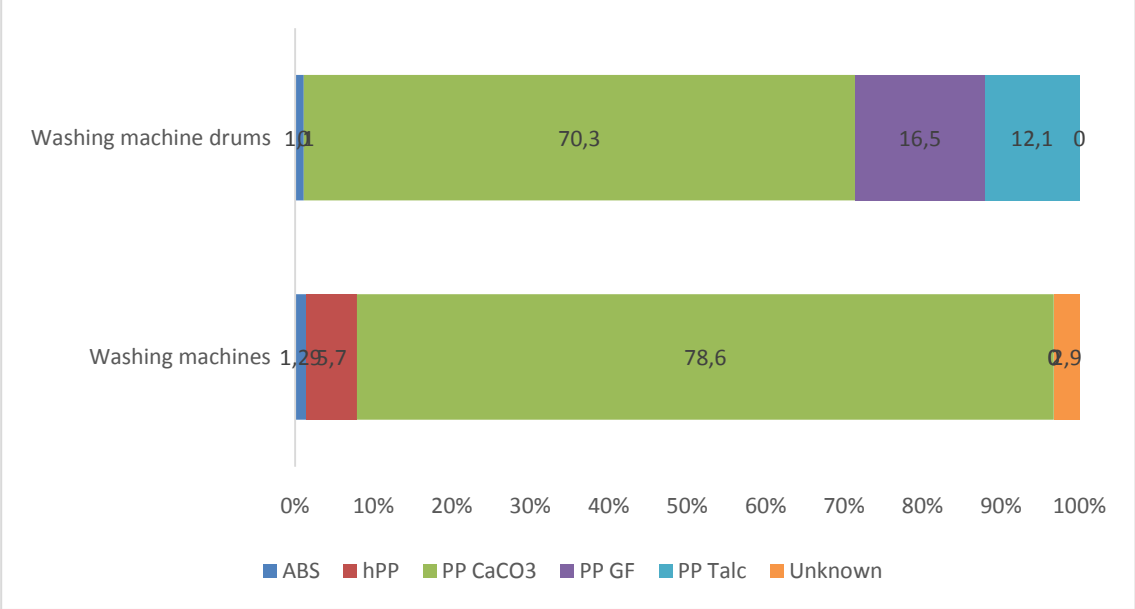

Figure 6.4. Polymeric composition of washing machines and washing machine drums

6.2.2.2 Discussion

Filled PP is the main constituent in both streams. However, washing machine drums contain a fraction of glass-fiber filled PP. This fraction is negligible in washing machines as a whole. Discussion with internal partners (Whirlpool) pointed out that the results are peculiar, as there is little difference in PP (filled or unfilled) content between the streams.

6.2.3 Small Household Appliance (SHA)

6.2.3.1 Results

Figure 6.5 shows the composition of the SHA WEEE stream as a whole. Figure 6.6 contains the experimental results for the three SHA products.

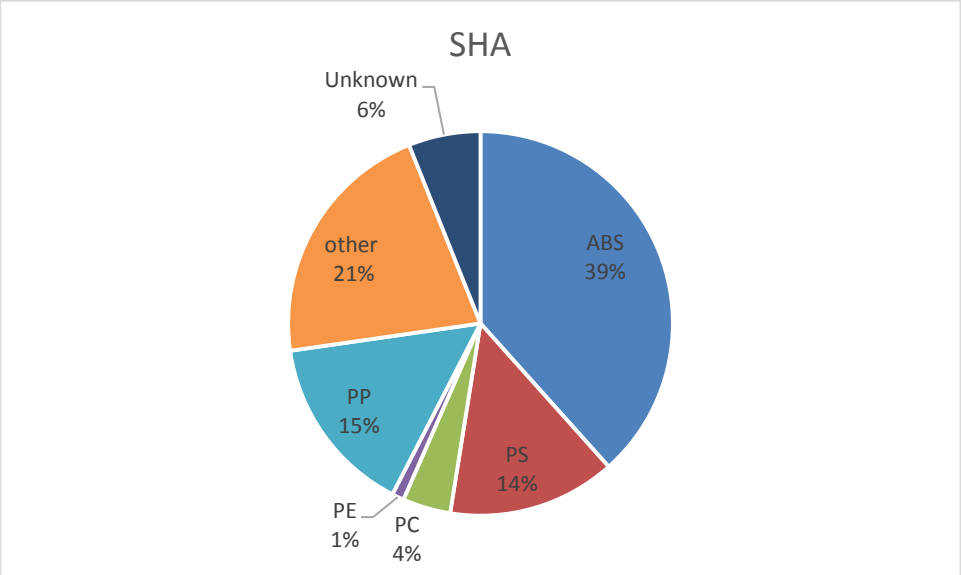

Figure 6.5. Composition of the SHA stream

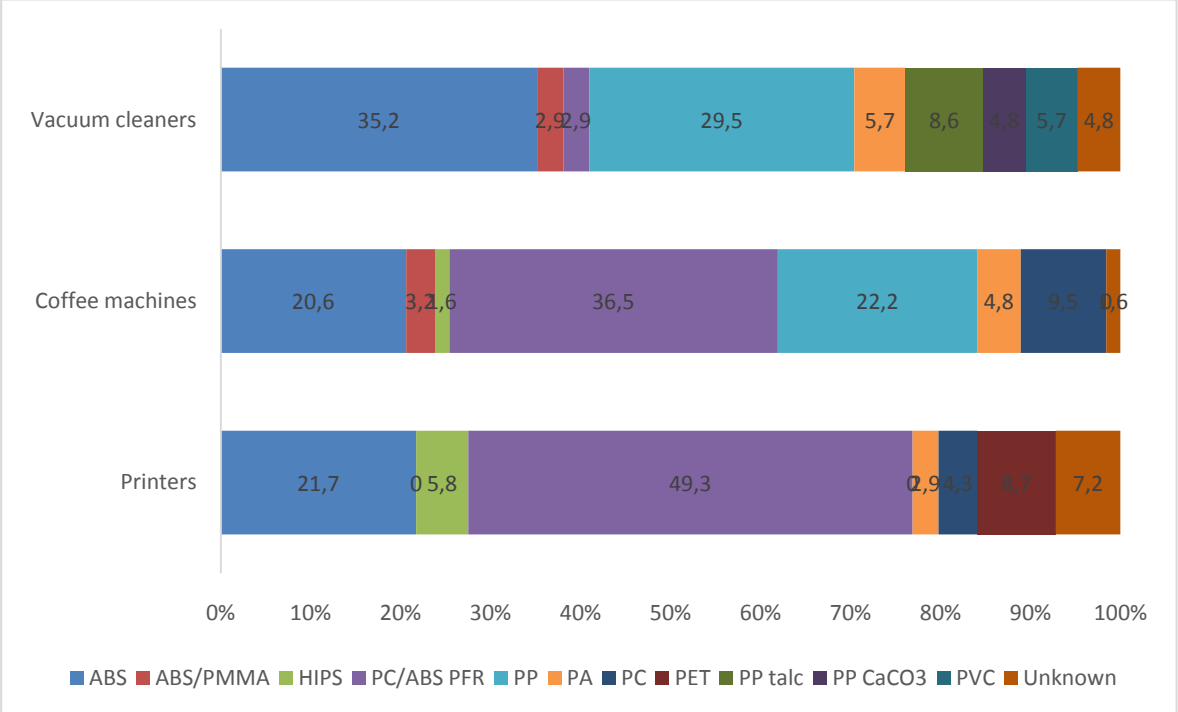

Figure 6.6. Polymeric composition of the three SHA category components

6.2.3.2 Discussion

The composition of each of the tested SHA products is highly complex. Particularly, the large percentages of unknown substances in vacuum cleaners and printers is problematic. Discussion with PolyCE partners (Phillips) indicated that the large presence of PC/ABS (which is an expensive polymer) in coffee machines is unexpected. A further investigation into this matter is a subject of Deliverable 4.4. The features derived in Chapter 5 can help reduce the complexity of the compositions. Figure 6.7 shows the heat-maps of the products before and after feature engineering. The figure indicates that the vacuum cleaners' polymers fall nicely into one feature. The compositions of printers and coffee machines fall almost evenly into two features, indicating a difficulty in sorting or blending them.

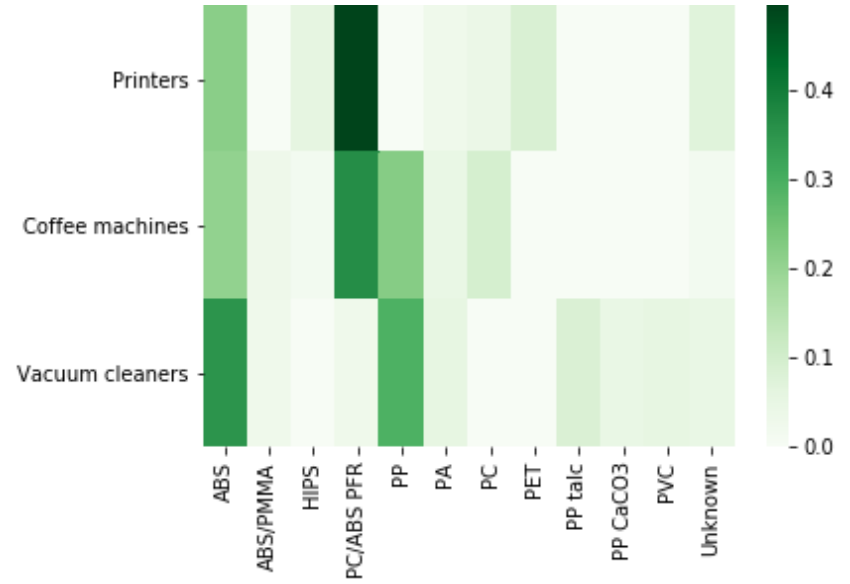

(a)

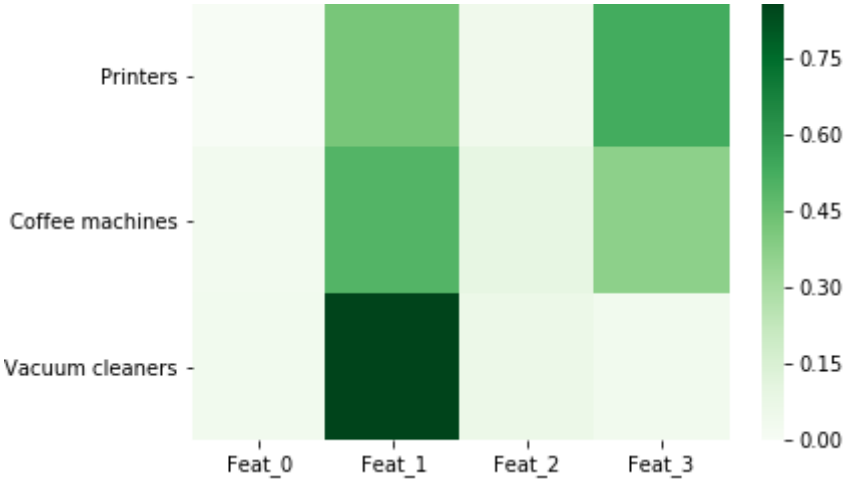

(b)

Figure 6.7. Heat-map of SHA data (a) before and (b) after feature engineering

For comparison, the heat-map after feature engineering for the entire SHA stream is depicted in Figure 6.8. Comparing figures 6.7 (b) and 6.8, one may conclude that a separate vacuum cleaners stream can improve recycling rates.

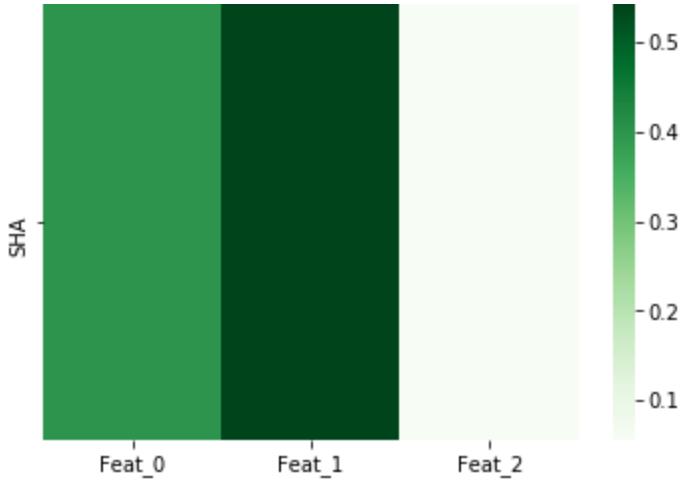

Figure 6.8. Heat-map of SHA stream after feature engineering

6.3 Clustering Policies

To test the profitability of clustering, experiments were performed for the three WEEE categories. The results are detailed below. Costs involved in implementing the clustering policies in practice were provided in Chapter 3.

6.3.1 Cooling and Freezing Equipment (C&F)

6.3.1.1 Entire C&F stream

Treating this stream as a whole, a net profit of $€137.55/tonne$ can be made by targeting PS and ABS by NIR and subsequently applying density-based separation with a density value of $0.98 g/cm^3$. Figure 6.9 shows the density spectra of the stream before and after NIR sorting.

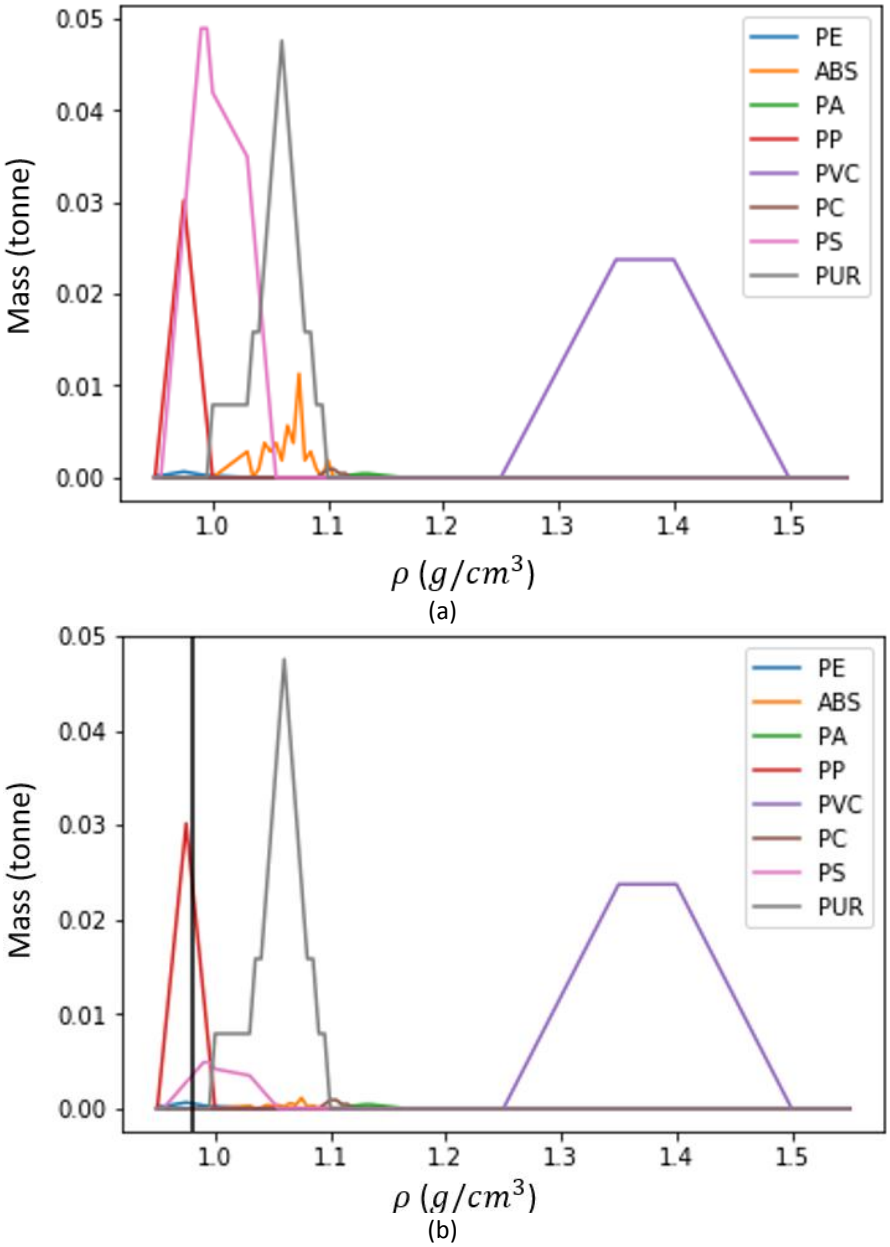

Figure 6.9. C&F waste stream (a) prior to NIR sorting (b) after NIR sorting. The black line indicates the density value at which density separation should take place.

Remark 5.1. *Note the following regarding Figure 6.9:*

1. *Parameter α (NIR efficiency) is very sensitive: the fraction of PS still present decreases with α. For the density-based sorting step, this means that the "line" could be moved to the right if α were larger, resulting in a higher PP yield;*
2. *Recyclate pricing parameters provided in Chapter 3 render PUR and PVC not resalable. Thus, everything with a density exceeding $0.98 g/cm^3$ is incinerated in this case study.*
3. *Contrary to the refrigerators stream, there is no data available regarding the degradation of the PS fraction in the C&F stream. Since refrigerators are the main component of the stream, it is safe to assume that 50% of the PS is substantially degraded. Without additional separation technology, this might make it necessary to incinerate the entire PS stream, reducing the profit to $€ - 77.53$.*

6.3.1.2 Refrigerator cluster

The optimal recycling strategy for a separate refrigerator stream is to target PS (degraded and non-degraded) and ABS by NIR. The degraded PS cannot be separated from the non-degraded PS. As such, the entire PS stream is unsuitable for recycling. After separating PS and PA by NIR, an almost pure HIPS fraction persists. Hence, no density separation is required. Figure 6.10 shows the density spectra of the refrigerators stream before and after NIR sorting.

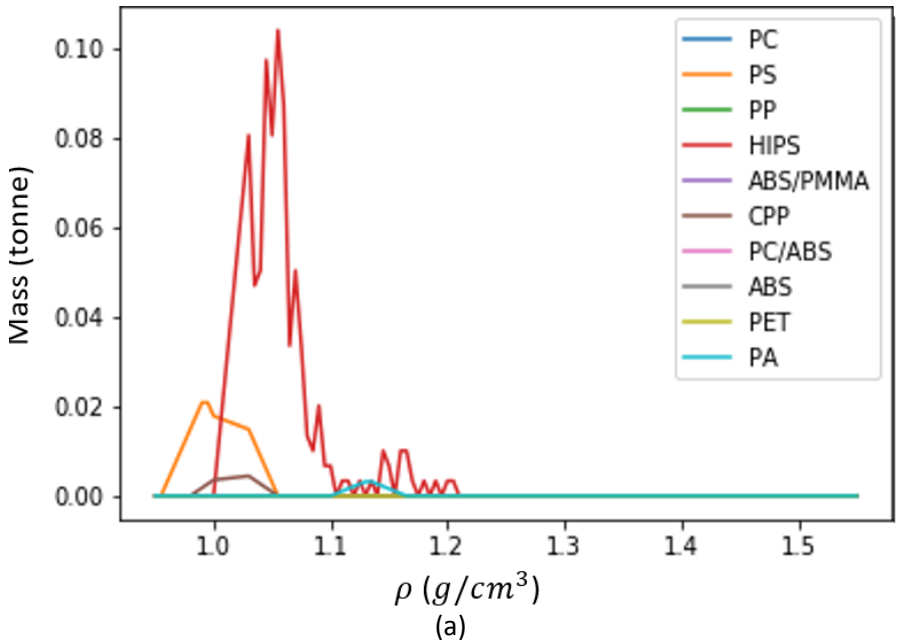

(a)

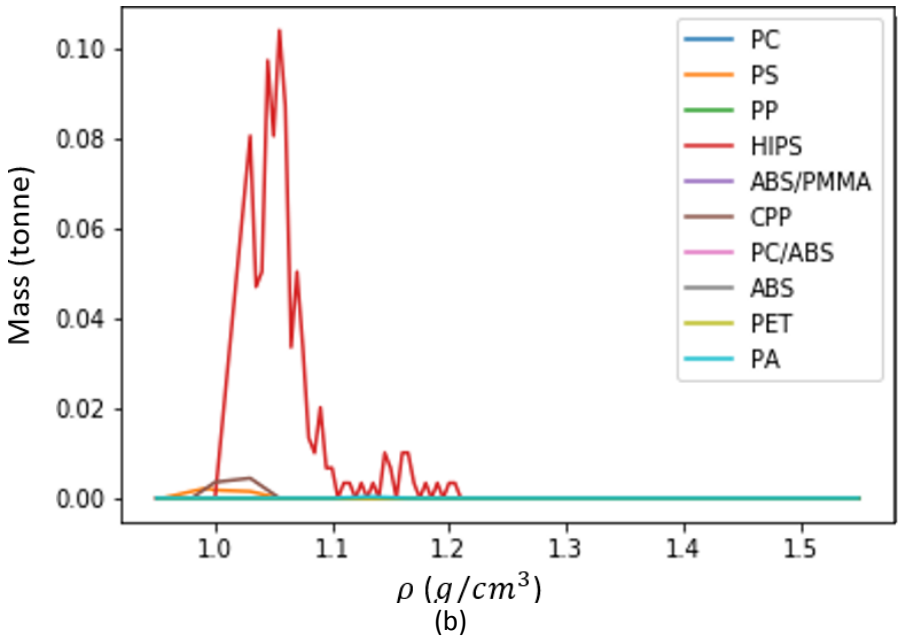

(b)

Figure 6.10. Refrigerator cluster (a) prior to NIR sorting (b) after NIR sorting

The profit generated during this stream is $€15.78/tonne$. Refrigerators constitute 93% of the C&F stream (see Table 3.2). Hence, the profit when treating refrigerators separately is $p_{clust} = 0.07 \cdot p_{C\&F} + 0.93 p_{Refr}$, where $p_{C\&F}$ and p_{refr} are the profits of the C&F stream and

the refrigerators cluster, respectively. Assuming that $p_{C\&F} = €-77.53/tonne$, the profit becomes $p_{clust} \approx €9.25/tonne$. Hence, the increase in profit from clustering, say Δp, is:

$$\Delta p = p_{clust} - p_{C\&F} = \frac{€\big(9.25 - (-77.53)\big)}{tonne} = €86.78/tonne$$

Note that $\Delta p < €420/tonne$, where the latter quantity is the added unit cost of carrying out the clustering operation. Hence, a dedicated refrigerator cluster results in a net loss of

$$\frac{€(\Delta p - 420)}{tonne} = €-333.22/tonne$$

So that the investment is not profitable.

6.3.1.3 Refrigerator cabinet clusters

One cluster

Supposing that 70% of refrigerator cabinets are transparent and 30% are white. Suppose further that the PS in the refrigerator cabinets is not degraded. Finally, suppose that white and transparent cabinets are treated in one cluster. The optimal sorting strategy then becomes as follows. Target the coPP by NIR. Subsequently, carry out one density-based sorting step at $1.04\ g/cm^3$. The unit profit becomes $€-103.65/tonne$, making further investigation unnecessary. The density spectra of the cluster prior and posterior to NIR are depicted in Figure 6.11.

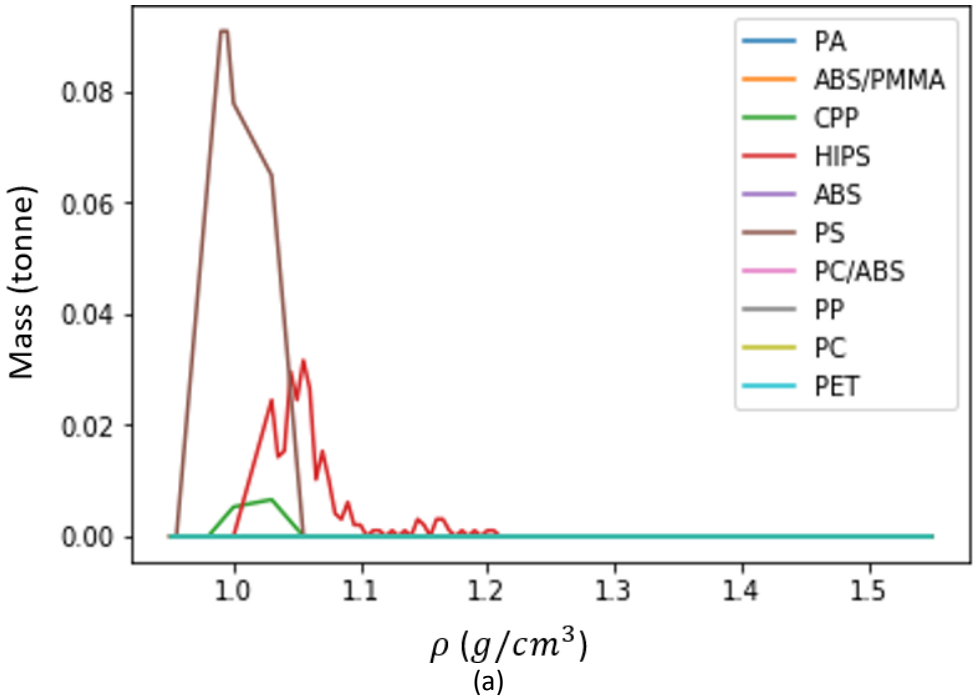

(a)

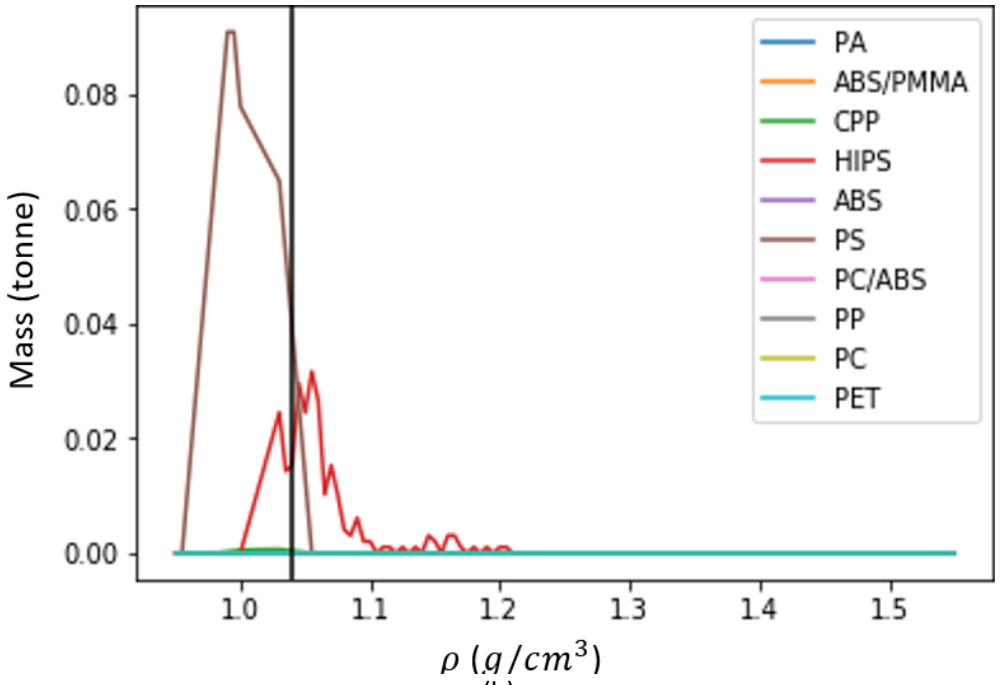

(b)

Figure 6.11. Refrigerator cabinet cluster (a) prior to NIR sorting (b) after NIR sorting. The black line indicates the density value at which density separation should take place.

Two clusters

Table 6.1 contains information regarding the clusters of white cabinets and transparent cabinets.

	White cabinet cluster	Transparent cabinet cluster
NIR targets	coPP; PS	-
Density values for separation $[g/cm^3]$	1.035	-
Unit profit $[€/tonne]$	201.00	140.00

Table 6.1. Experimental results for isolated cabinet clusters

While both clusters are highly profitable, they constitute only a small fraction of the total plastic mass of refrigerators. Assuming that cabinets constitute 5% of this mass, the total profit from isolating these clusters becomes

$$p_{cab} \approx 0.05(0.7p_{trans} + 0.3p_{white}) + 0.95p_{clust}$$

Where p_{cab} is the profit of carrying out the cabinet clustering, p_{trans} and p_{white} are the profits of the transparent and white cabinet clusters, respectively and p_{clust} is as in Section 1.1.2.1. Thus,

$$p_{cab} \approx \frac{€\left[0.05\left(0.7(140) + 0.3(201)\right) + 0.95(9.25)\right]}{tonne} \approx €87.94/tonne$$

Again, this unit profit cannot outweigh the clustering costs of $€420/tonne$ (the unit cost of dismantling and sorting).

6.3.2 Large Household Appliances (LHA)

Information regarding washing machine and washing machine drum treatment and unit profit is provided in Table 6.2. It is assumed that homoPP can be separated from coPP using NIR.

	Washing machines	Washing machine drums
NIR targets	PP	PP
Density values for separation $[g/cm^3]$	-	-
Unit profit $[€/tonne]$	407.14	544.00

Table 6.2. Experimental results for washing machines

Assuming that drums constitute 15% of the plastic composition of washing machines, the unit profit from targeting drums is roughly $€(0.85 \cdot 407.14 + 0.15 \cdot 544)/tonne \approx €427.67/tonne$. The net profit of clustering becomes $€(427.67 - 407.14)/tonne = €20.53/tonne$. Since the treatment of one tonne of washing machines takes well over an hour, this profit of $€20.53/tonne$ does not outweigh the $€60/h$ minimal treatment costs.

6.3.3 Small Household Appliances (SHA)

6.3.3.1 Entire SHA stream

Disregarding the unknown fraction (6%), a profit of $€278.32/tonne$ can be made by targeting PC and PP by NIR and subsequently applying density-based sorting at $\rho = 1.05\ g/cm^3$. Density spectra before and after NIR are included in Figure 6.12.

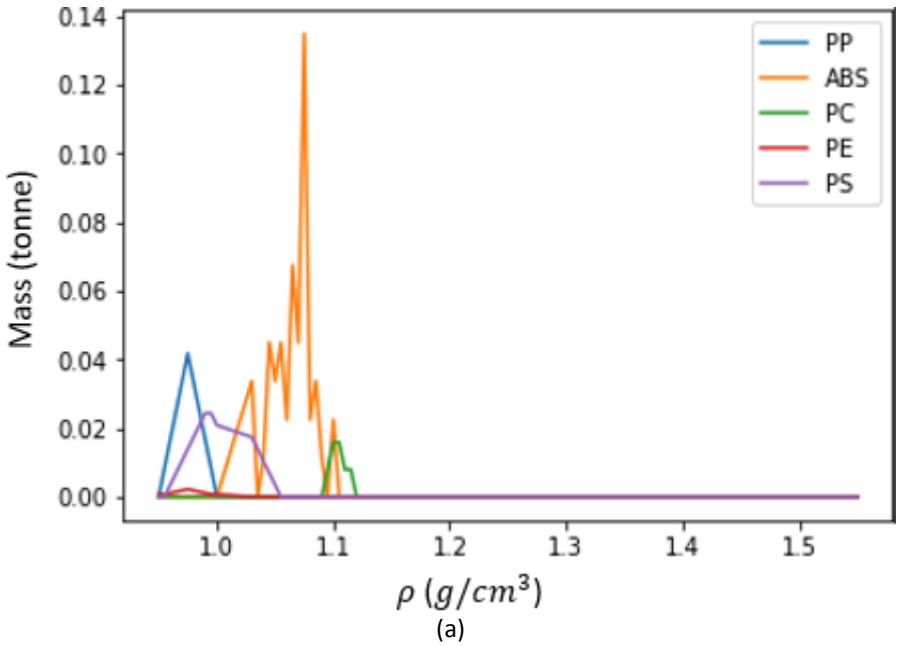

(a)

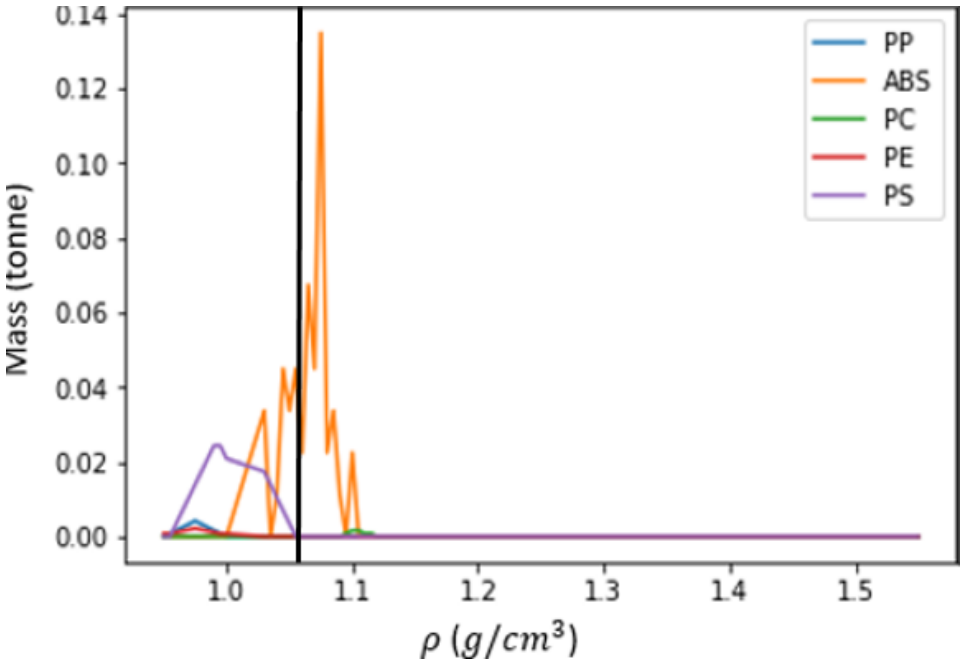

(b)

Figure 6.12. SHA stream (a) prior to NIR sorting (b) after NIR sorting. The black line indicates the density value at which density separation should take place.

6.3.3.2 Clustering of printers, coffee machines, vacuum cleaners

There are five possible clustering policies for a set of three products (five being the *Bell number* of three). Each clustering policy can be represented by a three-dimensional vector in $\{0,1,2\}^3$. The first entry in the vector represents printers, the second coffee machines and the third vacuum cleaners. That is:

$$(clust.of\ printers \quad coffee\ machines \quad vacuum\ cleaners)$$

The number in each entry represents the corresponding product belongs to. For instance, the vector $(0\ 1\ 1)$ represents a policy with two clusters, in which printers are in cluster 0 and coffee machines and vacuum cleaners are combined in cluster 1. Note that policies $(0\ 1\ 1)$ and $(1\ 0\ 0)$ are 'isomorphic' in the sense that they represent the same clustering policy, but the labels of the clusters are reversed. Due to the small number of clustering policies, the optimal policy is computed by enumeration. The results are included in Table 6.3. Relative masses of the products are taken as mentioned in Section 6.1.3.

Clustering policy	**Unit profit** $[€/tonne]$	**NIR targets** (Cluster 1; cl. 2; cl. 3)	**Density values** $[g/cm^3]$ (Cl. 1; cl. 2; cl. 3)
$(0\ 0\ 1)$	€69.63	-; PA	-; 1.00, 1.09
$(0\ 1\ 0)$	€3.59	PC; PA	-; -
$(1\ 0\ 0)$	€314.18	PC, PA; ABS	-; 1.00, 1.09
$(1\ 1\ 1)$	$€-40.94$	-	-
$(0\ 1\ 2)$	€383.06	ABS; PA; PA	-; -; 1.00, 1.09

Figure 6.3. Information regarding all possible clustering policies

So that the proposal based on the currently available data and estimations is to cluster each of the products individually. Note that in the light of the observations made in Section 6.2.3.2, it is surprising that policy $(1\ 0\ 0)$ outperforms policy $(0\ 0\ 1)$. This can be explained by the observation that printers, with a mass percentage of $7.8\ wt\%$ in the SHA stream have a much larger presence than vacuum cleaners ($2.9\ wt\%$).

Combined, printers, coffee machines and vacuum cleaners account for $14.4\ wt\%$ of the SHA stream. Adopting policy $(0\ 1\ 2)$, the net profit from clustering (assuming the total SHA stream remains as in Section 1.3.3.1 after these items have been removed) is:

$$\begin{aligned}€(0.144 \times 383.06 + 0.856 \times 278.32)/tonne - €278.32/tonne &= 293.40 - €278.32 \\ &= €15.08/tonne\end{aligned}$$

The additional labor costs were estimated at $€10/tonne$ to $€15/tonne$. Hence, the sampling campaign is not sufficiently profitable to break even with an initial investment of $€30{,}500$. However, if only vacuum cleaners are sorted,

$$€(0.029 \times 953.13 + 0.971 \times 278.32)/tonne - €278.32/tonne = €19.57/tonne$$

making the investment slightly more interesting. Assuming that the annual throughput of an MRF is $25 \cdot 10^3\ tonnes/year$, the annual net profit becomes

$$\frac{25 \cdot 10^3\ tonne}{year} \times \left(\frac{€(19.57 - 15)}{tonne}\right) = €114{,}250/year$$

so that the initial investment reaches a break-even point after less than four months. A dedicated vacuum cleaner cluster may therefore be worth the effort. Note that this is exactly the cluster obtained in Section 6.2.3.2 through mere inspection of the derived features. Thus, the case study solidifies the practical relevance of the methods introduced in Chapter 5.

7 Conclusion

Sound sampling campaigns were outlined for the collection of data regarding WEEE plastic content. A statistical method was also proposed for compliance testing that is also of use in PolyCE task 4.3 (Development of standard and systematic testing procedures for the different types of PCR to determine the PCR grade and to control quality consistency across the material value chain). Data were gathered regarding the following:

1. The distribution of products in key WEEE streams;
2. The polymeric compositions of products and their components;
3. The densities of materials.

Despite these efforts, the amount of data available is still limited.

A method was then derived to optimize the separation of the materials in a stream using near-infrared spectroscopy and density-based sorting. The method relies on dedicated heuristics, simulated annealing and a reformulation of a dynamic programming algorithm. Heuristics are used to find an interesting initial solution. This solution is then iteratively improved using a neighborhood comparison method. The involved operation costs have a particular structure that requires a computation through dynamic programming. It is worth pointing out that NIR was treated as a proxy for the set of non-density based sorting techniques applied in an MRF. Very little has been disclosed regarding the structure of actual MRFs over the course of the project or in literature. Modeling assumptions, however, are justified by the abundance and relative ease of density-based separation methods in practice.

Subsequently, clustering methods for product components were developed. The involved features rely on graph colorings. Outliers were detected using an isolation forest. Interestingly, in the light of the demonstrator cases, the developed features anticipated the most promising clustering policy (as computed by brute-force). This indicates that the feature engineering techniques are suitable for clustering applications in a practical setting.

The developed methods were applied in a case study involving three product component categories: cooling and freezing equipment, large household appliances and small household appliances. Data regarding the compositions of these categories in terms of products were used to identify key products. FTIR analyses for these products were then carried out to determine their polymeric composition. These data were used to analyze optimal clustering strategies for the distinct WEEE categories. Results indicated that the clustering of refrigerator drawers is a viable strategy for improved HIPS recovery. Likewise, the clustering of washing machine drums (separately from the remaining washing machines) helped recover more PP. Nonetheless, these strategies were not financially profitable. Computational experiments with the three main constituents of the small household appliances waste stream indicated that vacuum cleaners consist primarily out of ABS and PP. Separating them from the larger small household appliances stream may very well be profitable for WEEE material recycling facilities.

REFERENCES

[1] Eurostat, (2018). *Waste statistics - electrical and electronic equipment*. Retrieved from http://ec.europa.eu/eurostat/statistics-explained/index.php/Waste_statistics_-_electrical_and_electronic_equipment#Context, May 22, 2018

[2] Widmer, R., Oswald-Krapf, H., Sinha-Khetriwal, D., Schnellmann, M., Boni, H., (2005). *Global Perspectives on E-Waste. Environmental Impact Assessment Review* 25(5), pp. 436 – 458.

[3] European Commission, (2007). *Plastics Composition of WEEE and Implications for Recovery*. Retrieved from http://ec.europa.eu/environment/integration/research/newsalert/pdf/63na4_en.pdf, May 15, 2018.

[4] Cui, J. and Forssberg, E. (2003). Mechanical Recycling of Waste Electric and Electronic Equipment: A review. *Journal of Hazardous Materials* B99, pp. 243 – 263.

[5] Buekens, A. and Yang, J., (2014). Recycling of WEEE Plastics: A review. Journal of Material Cycles Waste Management 16, pp. 415 – 434.

[6] European Parliament and Council (2012). Directive 2012/19/EU of the European Parliament and of the Council of 4 July 2012 on waste electrical and electronic equipment (WEEE) Text with EEA relevance. Obtained from https://eur-lex.europa.eu/eli/dir/2012/19/oj, February 25, 2019.

[7] Accili, A., Campadello, L. Vincenti, N., Amadei, A., Arienti, G. and Sala, M. (2019). *Quantification of Material Flows Along the Entire Chain*. PolyCE report.

[8] Peeters, J.R., Vanegas, P., Kellens, K., Wang, F., Huisman, J. Dewulf, W. and Duflou, J.R. (2015). Forecasting Waste Compositions: A case study on plastic waste of electronic display housings. *Waste Management* 46, pp. 20 – 39.

[9] Delgado, C. and Stenmark, Å. (2005). Technological reference paper on recycling plastics. *VERC Deliverable Report*.

[10] WRAP (2009)., Separation of mixed weee plastics. *WRAP Report*.

[11] maisel, F., Rotter, V.S., Schneider-Ramelow, M. (2019). Influence of the Particle Size on the Plastic Recyclability of Plastic Fractions from WEEE Treatment. Master Thesis, Technische Universität Berlin; Fraunhofer IZM.

[12] Gent, M., Menendez, M., Toraño, J. and Diego, I. (2009). Recycling of plastic waste by density separation: Prospects for optimization. *Waste management and Research*, vol. 27, p. 175 187.

[13] Marques, G. and Tenório, J. 92000). Use of froth flotation to separate pvc/pet mixtures. *Waste Management*, vol. 20.

[14] American Chemistry Council, (2011). Demingling the mix: An assessment of commercially available automated sorting technology.

[15] Kessler, A, (2015). Plastics Packaging Design for Recycling: Background and Recommendations. Suez report.

[16] Van Kooy, L., Mooij, M. and Rem, P. (2004). Kinetic gravity separation. *Physical Seperation in Science and Engineering*, vol. 13, no. 1, pp. 25 – 32.

[17] Petridis, N., Stiakakis, E., Petridis, K. and Dey, P. (2015). Estimation of computer waste quantities using forecasting techniques. *Journal of Cleaner Production*, vol. 112, p. 3072 3085.

[18] Peeters, J.R., Altamirano, D., Dewulf, W. and Duflou, J.R. (2017). Forecasting the composition of emerging waste streams with sensitivity analysis: A case study for photovoltaic (pv) panels in flanders. *Resources, Conservation and Recycling*, vol. 120, pp. 14 – 26.

[19] Maris, E., Botane, P., Wvrer, P. and Froelich, D. (2015). Characterizing plastics originating from weee: A case study in france. *Minerals Engineering*, vol. 76, pp. 28 – 37.

[20] Vanegas, P., Peeters, J.R., Cattrysse, D., Dewulf, W. and Duflou, J.R. (2017). Improvement potential of today's weee recycling performance: The case of lcd tvs in Belgium. *Frontiers of Environmental Science and Engineering*, vol. 11, no. 5, pp. 265 – 269.

[21] Menad, N., Guignot, S., and Van Houwelingen, J. (2013). New characterisation method of electrical and electronic equipment wastes. *Waste Management*, vol. 33, no. 3, pp. 706 – 713.

[22] Bovea, M.D., Pérez-Belis, V., Ibáñez-Forés, V., Quemades-Beltrán P. (2016). Disassembly properties and material characterisation of household small waste electric and electronic equipment. *Waste Management*, vol. 53, pp. 225 - 236.
[23] Peeters, J.R., Vanegas, P. Tange, L., Van Houwelingen, J., Duflous, J.R. (2014). Closed Loop Recycling of Plastics Containing Flame Retardants. *Resources, Conservation and Recycling* vol. 84, pp. 35 – 43.
[24] Mba polymers, (2017). http://www.mbapolymers.com/home/complex-waste-plastics-recycling-wish-list Retrieved: December 2017.
[25] Balde, C.P., Kuehr, R., Blumenthal, K., Fondeur Gill, S., Kern, M., Micheli, P., Magpantay, E. and Huisman, J., (2015). E-Waste Statistics: Guidelines on classification, reporting and indicators. United Nations University.
[26] World Customs Organization, (2019). What is the Harmonized System (HS)?. Retrieved from http://www.wcoomd.org/en/topics/nomenclature/overview/what-is-the-harmonized-system.aspx, December 20, 2019.
[27] Gy, P., (2004). Sampling of Discrete Materials – A new introduction to the theory of sampling: I. Qualitative approach. *Chemometrics and Intelligent Laboratory Systems*.
[28] Gy, P., (2004). Sampling of Discrete Materials: II. Quantitative – Sampling of zero-dimensional objects. approach. *Chemometrics and Intelligent Laboratory Systems*.
[29] Gy, P., (2004). Sampling of Discrete Materials: III. Qualitative approach – Sampling of one-dimensional objects. *Chemometrics and Intelligent Laboratory Systems*.
[30] Van de Vaart, A.W., (2010). *Mathematische Statistiek*. Universiteit van Amsterdam.
[31] Walpole, R.E., Myers, R.H., Myers, S.L. and Ye, K.E., (2012). *Probability and Statistics for Engineers and Scientists*. Pearson.
[32] Cohen, J., (1977). *Statistical Power Analysis for the Behavioral Sciences*. Academic Press.
[33] Gillet, R., (1996). Sample Size Determination in a Chi-Squared Test Given Information From an Earlier Study. *Journal of Educational and Behavioral Statistics*.
[34] Banning, R., Camstra, A. and Knottnerus, P., (2010). *Steekproeftheorie: Steekproefontwerpen en Ophoogmethoden*. Centraal Bureau voor de Statistiek (CBS).
[35] Maisel, F., Chancerel, P., Dimitrova, G., Emmerich, J., Nissen, N.F. and Schneider-Ramelow, M., (2019). *Preparing WEEE plastics for recycling how optimal particle sizes in pre-processing can improve the separation efficiency of high quality plastics*. Forthcoming.
[36] Wagner, F., Peeters, J.R., De Keyzer, J., Janssens, K., Duflou, J.R. and Dewulf, W., (2019). Towards a More Circular Economy for WEEE Plastics – Part A: Development of innovative recycling strategies. *Waste Management* vol. 100, pp. 269 – 277.
[37] Wagner, F., Peeters, J.R., De Keyzer, J., Janssens, K., Duflou, J.R. and Dewulf, W., (2019). Towards a More Circular Economy for WEEE Plastics – Part B: Assesment of the technical feasibility of recycling strategies. *Waste Management* vol. 96, pp. 206 – 214.
[38] Gutowski, T., Dahmus, J., Albino, D. and Branham, M. (2007). Bayesian material separation model with applications to recycling systems. *International Symposium on Electronics and the Environment*.
[39] Wolf, M., Colledani, M., Gershwin, S. and Gutowski, T. (2010). Modeling and design of multi-step separation systems. *IEEE Proceedings of the Symposium on Sustainable Systems Technology*.
[40] Wolf, M. (2011). *Modeling and Design of Material Separation Systems with Applications to Recycling*. Massachusetts Institute of Technology.
[41] Wolf, M., Colledani, M., Gershwin, S. and Gutowski, T. (2013). A network flow model for the performance evaluation and design of material separation systems for recycling. *IEEE Transactions on Automation Science and Engineering*, 10(1), pp. 65 – 75.
[42] Testa, M., (2015). *Modeling and Design of Material Recovery Facilities: Genetic Algorithm Approach*. Massachusetts Institute of Technology.
[43] Sodhi, M.S., Young, W.A. and Knight, W.A., (1999). Modeling Material Separation Processes in Bulk Recycling. *International Journal of Production Research* 37(10), pp 2239 – 3353.
[44] Hurink, J., (1998). *Solving Complex Optimization Problems by Local Search*. Habilitationsschrift, Universität Osnabrück.
[45] Cormen, T., Leiserson, C., Rivest, R., and Stein, C. (2009). *Introduction to Algorithms*. Cambridge, MA: The MIT Press.
[46] Spieksma, F. (2016). *Lecture Notes Optimization: Special Topics*. Katholieke Universiteit Leuven.

[47] Wilson, R.J. (2010). *Introduction to Graph Theory*. Harlow, England: Prentice Hall.
[48] Liu, Fei Tony, Ting, Kai Ming and Zhou, Zhi-Hua (2013). Isolation-based anomaly detection. *ACM Transactions on Knowledge Discovery from Data (TKDD)* 6.1.
[49] Mitchell, T.M. (1997). *Machine Learning*. McGraw-Hill Companies Inc.

Appendix A. Data Collection and Analysis

Appendix A.1. Meta-Data Sheet Batch Sampling

(To be anonymized)		
Company		(name)
Date sample sent		(dd-mm-yyyy)
Date sample received	*To be entered by KU Leuven*	(dd-mm-yyyy)
Sample identification code	*To be entered by KU Leuven*	(unique sample code)
Full address of the plant		(address)
E-mail address contact person		(e-mail)
Phone number contact person		(phone number)
General Description		
(Used confidentially)		
Product categories:		
Small household appliances		(yes/no)
Large household appliances		(yes/no)
Television screens		(yes/no)
Monitors		(yes/no)
Cooling and freezing equipment		(yes/no)
Washing machines and dryers		(yes/no)
Other, please specify		(description)
Sample size		
Weight of sample sent to KU Leuven		(mass in kg)
Total weight in sampling campaign		(mass in kg)
Manual sorting		
Components manually removed pre-shredder		(component(s) description)
Components manually removed post-shredder		(component(s) description)
Size reduction processes:		
Knife shredder		(yes/no)
Hammer mill		(yes/no)
Granulator		(yes/no)
Crusher		(yes/no)
Other, please specify		(description)
Sieving:		
Sieving size(s)		(max mesh size in mm)
Metal sorting technology:		
Float/sink method		(yes/no)
Magnetic roller		(yes/no)
Eddy currents		(yes/no)
Other, please specify:		(description)
Plastic sorting technology:		
Float/sink method		(yes/no)
(Hydro)cyclone/centrifugal sorting		(yes/no)

Wet jig (shaking table)	(yes/no)
Dry jig (shaking table)	(yes/no)
Other density-based method (please specify)	(description)
(Froth) Flotation	(yes/no)
X-ray sorting	(yes/no)
Polarized UV-light sorting	(yes/no)
Other optical method	(description)
Dispersive Fourier Transform	(yes/no)
Diffraction grating Fourier Transform	(yes/no)
Laser-induced breakdown spectroscopy (LIBS)	(yes/no)
Laser-induced plasma spectroscopy (LIPS)	(yes/no)
Thermal infrared spectroscopy (TIR)	(yes/no)
Mid-infrared spectroscopy (MIR)	(yes/no)
Near-infrared spectroscopy (NIR)	(yes/no)
Other spectrographic method (please specify)	(description)
Electrostatic sorting	(yes/no)

Appendix A.2. Power Table Chi-Squared Test

	Effect size								
n_i	0.1	0.2	0.3	0.4	0.5	0.6	0.7	0.8	0.9
25	1	2	5	10	19	32	49	67	81
30	1	3	6	13	25	42	61	78	90
35	1	3	7	16	31	51	71	87	95
40	1	3	8	19	37	60	79	92	98
45	2	4	10	23	44	67	86	95	99
50	2	4	12	27	50	74	90	98	
60	2	5	15	35	62	85	96	99	
70	2	6	19	44	72	91	98		
80	2	7	23	52	81	95	99		
90	2	8	28	60	87	98			
100	2	10	32	67	91	99			
120	3	13	42	78	96				
140	3	16	51	87	99				
160	3	19	60	92					
180	4	23	67	95					
200	4	27	74	98					
250	5	37	87						
300	7	48	94						
350	8	58	97						
400	10	67	99						
500	13	81							
600	18	90							
700	22	95							
800	27	98							
900	32	99							
1000	37								

Table A.2. Table for chi squared test for 7 degrees of freedom and $\alpha = 0.01$. Recall that the values in the table are powers (that is: the chance of avoiding a type-II error). The table is taken from [Cohen].

Appendix A.3. Material composition of product components

Product and component	ABS	ABS/ PMMA	HIPS	HIPS/ PPE	PA	PC/ABS	PP	Unknown	No. samples
Dishwashers front panel	0.92							0.08	20
Washing machines front cover	0.95					0.05			20
Washing machines drum							1		20
Washing dryers front cover	1								1
Refrigerator door			1						20
Refrigerator interior			0.95					0.05	39
Refrigerator cabinets			0.95					0.05	39
Freezers interior	0.08		0.92					0.13	49
Food equipment container	1								1
Food equipment side	0.5			0.5					2
Hot water equipment back cover	1								1
Hot water equipment water boxes			1						1
Hot water equipment front	1								1
Hot water equipment side	0.5					0.5			2
Vacuum cleaners back cover	1								1
Vacuum cleaners front cover			1						1
Vacuum cleaners front removable drawer	1								1
Hair dryers main body						1			1
Small IT back cover	0.67		0.33						3
Small IT back side		1							1

Table A.3. Polymer compositions of product components (repeated on next page). Empty cells indicate an absence of the material in the corresponding column in the product in the corresponding row.

Product and component	ABS	ABS/ PMMA	HIPS	HIPS/ PPE	PA	PC/ ABS	PP	Unknown	No. samples
Small IT top cover	0.33		0.33	00	0.33				3
Laptops bottom cover					1				9
Laptops display frame		0.13				0.87			8
Laptops keyboard cover		0.5		0.1		0.4			10
Laptops maintenance cover						1			1
Laptops top cover		0.25	0.13			0.63			8
Laptops back cover						1			1
Printers base cover			1						1
Printers housing	0.32		0.27			0.41			22
Printers interior	0.38		0.56	0.06					16
Printers side			1						1
Printers top cover	0.5		0.5						2
CRT monitors back cover	0.63		0.01	0.05		0.32			146
LCD monitors back cover	0.58	0.02	0.27			0.13			158
Audio equipment back cover	0.33	0.33	0.33						3
Audio equipment base		0.25	0.75						4
Audio equipment side			1						1
Speakers side			1						1
CRT TV back cover	0.08		0.75	0.1	0.01	0.04	0.03		384
LCD TV back cover	0.09	0.07	0.43	0.13		0.27		0.01	777
LCD TV front cover	0.17	0.17				0.67			6
LED TV back cover	0.44		0.11			0.44			9
Led TV back cover higher part			1						1
LED TV back cover lower part			1						1
LED TV enclosure	1								1
LED TV front frame			1						1
LED TV stand	1								1
Special lamps side			1						1
Game consoles top cover						1			1
Cooled dispensers front panel						1			1

Table A.3. (continued)

Appendix B. Complete Density Overlap Table

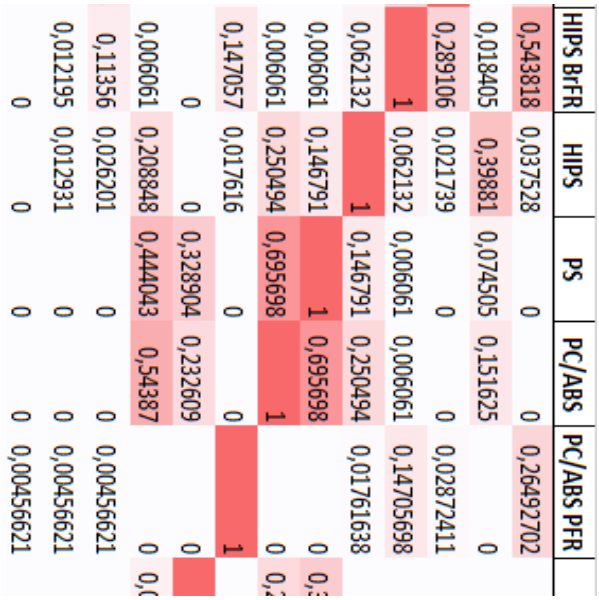

HIPS BrFR	HIPS	PS	PC/ABS	PC/ABS PFR	
0,543818	0,037528	0	0	0,26492702	
0,018405	0,39881	0,074505	0,151625	0	
0,289106	0,021739	0	0	0,02872411	
1	0,062132	0,006061	0,006061	0,14705698	
0,062132	1	0,146791	0,250494	0,01761638	
0,006061	0,146791	1	0,695698	0	0,3
0,006061	0,250494	0,695698	1	0	0,2
0,147057	0,017616	0	0	1	
0	0	0,328904	0,232609	0	0,(
0,006061	0,208848	0,444043	0,54387	0	
0,11356	0,026201	0	0	0,00456621	
0,012195	0,012931	0	0	0,00456621	
0	0	0	0	0,00456621	

Appendix C. List of Acronyms

ABS	Acrylonitrile butadiene styrene
C&F	Cooling and Freezing Equipment
CI	Confidence Interval
DBS	Density-Based Sorting
DP	Dynamic Programming
EEE	Electric and Electronic Equipment
FTIR	Fourier Transform Infrared Spectroscopy
GF	Glass fiber
HIPS	High impact polystyrene
LHA	Large Household Appliances
MRF	Material Recovery Facility
PAO	Proportional Area of Overlap (with respect to the total area) in normalized density spectra
PBT	Polybutylene terephthalate
PC	Polycarbonate
PE	Polyethylene
PET	Polyethylene terephthalate
PMMA	Polymethyl methacrylate
POM	Polyoxymethylene
PP	Polypropylene
PPE	Polyphenyl ether
PS	Polystyrene
PVC	Polyvinyl chloride

SA	Simulated Annealing
SAN	Styrene-acrylonitrile
SHA, sWEEE	Small Household Appliances (as a WEEE category)
SSE	Sum of Squared Errors
TV&S	Television sets and screens/monitors
WCR	Worst-Case-Ratio
WEEE	Waste Electric and Electronic Equipment